Journal of Building Engineering 57 (2022) 104801

Contents lists available at ScienceDirect

Journal of Building Engineering

journal homepage: www.elsevier.com/locate/jobe

Seismic assessment of the XX century masonry buildings in Florence: Vulnerability insights based on urban data acquisition and nonlinear static analysis

Vieri Cardinali [a,*], Marco Tanganelli [a], Rita Bento [b]

[a] Department of Architecture, University of Florence, Florence, Italy
[b] CERIS Instituto Superior Técnico, University of Lisbon, Lisbon, Portugal

ARTICLE INFO

Keywords:
Existing buildings
Masonry buildings
Seismic assessment
Nonlinear static analysis
EF discretization
Fragility curves

ABSTRACT

This paper deals with the seismic vulnerability assessment of modern masonry buildings in Florence, Italy. The work focuses on the XX century masonry structures realized before seismic codes. The research is divided into two main distinct phases: i) the acquisition of the main geometrical and structural information at the urban scale; ii) the selection of a representative model to execute an analytical assessment. The first part of the work represents a cognitive phase based on archive research and the collection of the buildings, which allowed the architectural and structural identification of over 300 structures. The second part of the work represents an analytical phase targeted at deriving fragility curves. A real case study representative of the simple block typology with two apartments per floor and a central stairwell has been selected and a probabilistic framework based on nonlinear static analysis has been performed. The analytical conclusions of the research point out a significant vulnerability of these structures, mainly ruled by a weak-piers-strong-spandrels behaviour. For the Life Safety limit state (SLV), around 40% of probability to having DL4 and 40% reaching DL5 are expected. The paper presents the results in terms of generic outcomes providing indications useful for the uncertainty's treatment and the engineering practice.

1. Introduction

The seismic risk assessment of urban areas constitutes an important issue in many parts of our planet. This is related to the intrinsic hazard of our planet, combined with the vulnerability and the exposure of cities and territories [1]. Within the three risk's components the vulnerability of the assets represents the parameter where is easier to intervene through mitigation measures. Due to this, the seismic vulnerability assessment plays a crucial role in the evaluation - and mitigation - of the seismic risk. Although National and International codes [2–4] provide the necessary tools to design new constructions, the vulnerability of existing buildings is more difficult to be defined. Considering the existing urban stock, the safety of the places where people live, the houses, is primarily important [5–11]. Several methodologies define the seismic vulnerability of the existing structures according to different approaches [12–15]. As regards Italy, the significant seismic hazard of the territory is combined with complex, heterogenous and vulnerable constructive traditions. In this context, the seismic codes became effective only recently, so the majority of the constructions have been realized without considering the effects of horizontal actions [16].

* Corresponding author.
E-mail address: vieri.cardinali@unifi.it (V. Cardinali).

https://doi.org/10.1016/j.jobe.2022.104801
Received 8 December 2021; Received in revised form 23 May 2022; Accepted 9 June 2022
Available online 16 June 2022

The earthquakes that occurred in the last decades (Molise 2002, L'Aquila 2009, Emilia Romagna 2012, Central Italy 2016) marked the vulnerability of the residential buildings where people live [17–19]. Masonry structures, due to their number and age, deserve a particular attention. Data updated in 2001 denounce that 61.5% of residential buildings is made by masonry buildings [20]. Besides the monumental buildings, which received special value for their cultural and architectural importance, most part of masonry buildings is represented by residential ones. The seismic protection of the cities and their population deals with preserving and conserving the historical heritage of human development in urban areas.

This work deals with the seismic vulnerability assessment of the XX century masonry buildings realized in Florence. Although the

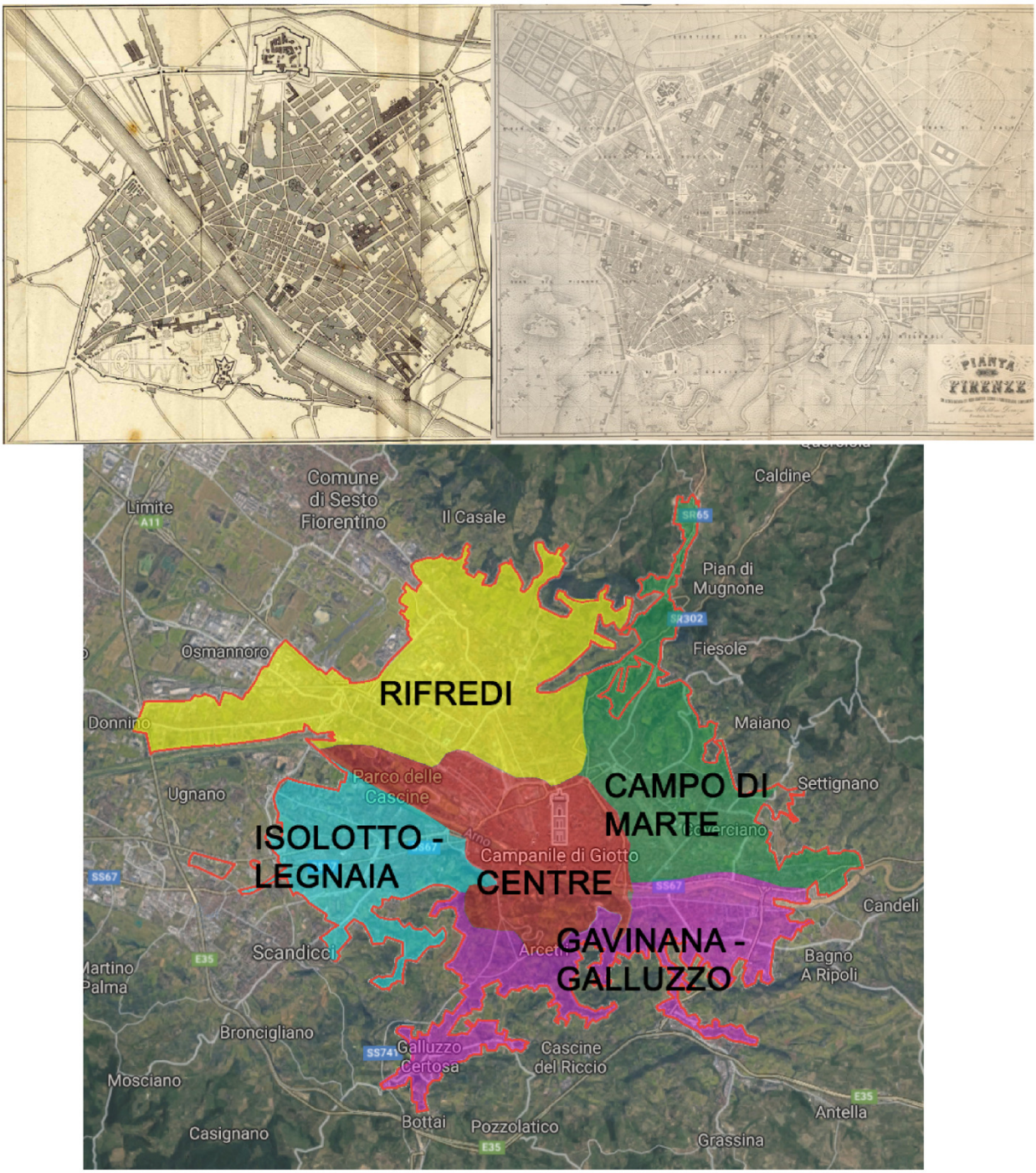

Fig. 1. The Florence city maps. On the left: a 1853 city map with the city enclosured into the town walls. On the right: the city in 1872. Below: the Contemporary city with its main districts.

city of Florence is worldwide famous as the Capital of Renaissance for its historical and artistic heritage, most of the contemporary city is constituted by external districts developed during the last two centuries. Florence is classified seismic zone from 1982, so most part of its urban stock has been realized without seismic criteria [21]. The area is characterized by a moderate telluric activity documented since the Medieval time; historical earthquakes were estimated around 5 of the Richter local magnitude scale (ML), and their epicenters were located around Florence (Mugello 1542 and 1919, Impruneta 1456 and 1895, Valdarno 1770). The most severe earthquakes of the area occurred in 09/28/1453 and 05/18/1895, both estimated at grades VII-VIII Mercalli-Cancani-Sieberg (MCS) level [22,23].

The XX century masonry buildings have been targeted for this research due to different reasons: i) the last significant earthquake that occurred in Florence hit the area only in 1895; therefore, the residential stock made in the XX century has never been subjected to relevant ground motions; ii) the masonry buildings realized in the last 100 years present common characteristics since the constructive methodologies became more standardized than before. The first part of the research concerns a cognitive approach aimed at the collection and characterization of the buildings. Archive research has been conducted, and several architectural and structural features have been listed to identify the building taxonomy. Then, an analytical procedure based on nonlinear static analysis has been defined and applied to a selected case study for in depth analysis following a probabilistic approach. The outcomes of the research provide

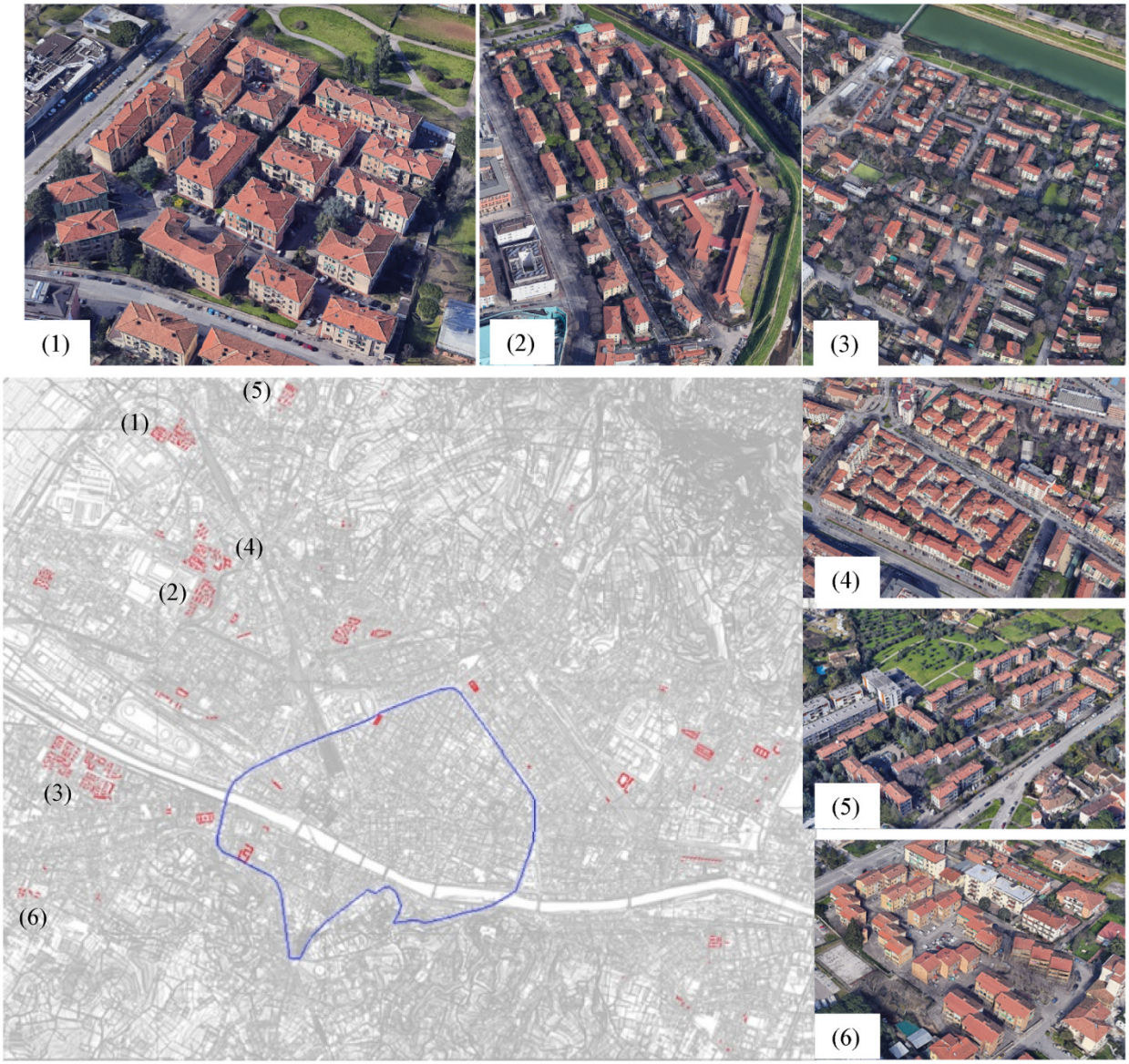

Fig. 2. Below, on the left, the map for the city of Florence. In red, the spatial distribution of the collected public housings; the blue line indicates the perimeter of the historical center of the city. In the top and right frames: aerial views of several XX century residential interventions in Florence. (For interpretation of the references to colour in this figure legend, the reader is referred to the Web version of this article.)

vulnerability insights extendable to a wider building class, allowing useful practice-oriented indications for the investigation of similar cases.

1.1. The seismic behaviour of modern masonry buildings

The masonry structures realized during the XX century in Italy are usually characterized by regular configurations of walls, rigid/semi-rigid slabs and perimetral ring beams. They present common features, especially referring to the in-plane seismic response of the structures [24]. The presence of rigid diaphragms allows a box-behaviour if the connections between the diaphragms and the walls are adequate [25,26]. Due to the diaphragms, the local mechanisms are generally avoided, and the entire structure participates to the structural performance of the building. Sandoli and Calderoni [27] consider the URM buildings from their capacity resist to horizontal actions, dividing the structures in three consequential classes: ancient masonry buildings (AMB), improved-ancient masonry buildings (IMB) and modern masonry buildings (MMB). The first two typologies are referred to traditional masonry structures conceived following empirical concepts. In the first class (masonry buildings and wooden no-rigid slabs), the failure mechanisms are mainly activated by local phenomena. Considering the second class, the structures are improved by light interventions (steel tie-rods connections), overcoming the out-of-plane failures, and involving the in-plane resistance of the structures. The general in-plane capacity of these structures is usually referred to a strong-piers-weak-spandrels behaviour (SPWS). This building's behaviour is comparable to free cantilevers embedded at the ground level where the coupling effects are given by the spandrels. Finally, the third class is referred to modern buildings realized during the XX century in force of the legislations promoted since the first decades [28,29]. The latter are characterized by rigid diaphragms and ring beams that allow a global behaviour. In this third class, the out-of-plane mechanisms are generally avoided, and the in-plane capacities of the walls are involved.

In Switzerland, a series of studies conducted over the URM buildings with RC slabs provided indications for the behaviour of such type of structures, the modeling approaches, the code limits and retrofitting solutions, pointing out the needs for evaluation of such types of structures in the Swiss context [30,31]. Penna et al. [32] showed how, after the 2012 earthquake, a relevant number of modern structures well responded to the seismic event in the Emilia Romagna Region due to the limited number of storeys and their structural redundancy. Nonetheless, a limited number of buildings realized without seismic codes suffered extensive damage led by shear diagonal and bi-diagonal cracks at the ground floor. Recently, Calderoni et al. [33] presented an overview of the damage assessment of modern masonry buildings after L'Aquila earthquake, including public housing interventions (*IACP* buildings). The results point out a global behaviour of these structures under seismic load. However, they also express severe damage related to their reduced in-plane shear capacity. Valluzzi et al. [34] presented a terraced-house case study realized by the public housing institutions and hit by the Central Italy earthquake. Due to plan irregularities and heterogenous masonry typologies, the building pointed out a hybrid response, mostly a global one but with punctual out-of-plane failures.

1.2. The modern masonry buildings in Florence

The contemporary Florence hosts over 380 000 citizens and it is the chief town of a metropolitan area with over 1 million inhabitants. Considering only the municipality, the city counts 31 070 residential buildings. Within them, 24 308 structures are realized by masonry structures (78.2%). The rest of the houses is divided between 4840 RC constructions (15.5%) and 1110 buildings realized with different technologies (steel or wooden realizations) (6.3%). The most significant part of the Municipality was made during the XX century (Fig. 1), as the spread of the city started with the designation of Florence as Capital of Italy in 1865. After this episode, the town walls were demolished and replaced by new boulevards connecting the old city with the new perimetral districts. Later, other districts were erected in external areas during the 30's and after WWII up to the 70's. The development of Florence's outskirts has been affected by the standardization procedures developed in the last century and the architectural design introduced by the Modern

Table 1
Overview of the archive collections investigated for this work.

Archive source	Period	Technical documentation		Drawings	Drawing details
IACP/Ater	XIXth century	Literature documentation; aerial views, photos of the interventions	F	/	/
			W	/	/
			S	/	/
	IACP 30s	Literature documentation; aerial views, photos of the interventions	F	/	/
			W	●	/
			S	/	/
	INA-Casa/Gescal ('50s-'60s)	General relations; tender specifications; metric computations	F	/	●
			W	●	●
			S	●	/
Ferrovie dello Stato	RFI – between the two WWs (20s–50s)	General relations; tender specifications; metric computations, site quantifications	F	/	●
			W	●	●
			S	●	●
Archivio storico	30s	/	F	/	/
			W	●	/
			S	●	/
	INA-Casa/Gescal (50s–60s)	/	F	●	/
			W	●	/
			S	●	/

Movement. Comparing the last districts with the historic ones, regular structures characterize the new urban stock. In several cases, the proposed interventions regarded the contemporary erection of several isolated houses adopting few architectural schemes and design (Fig. 2) [21,35].

2. Urban data acquisition

Cognitive research has been carried out at the urban scale. The achieved knowledge allowed obtaining of the main structural and architectural features of the XX masonry building urban stock. To this aim, the public housing interventions have been selected for in-depth studies. In fact, Florence experienced a significant promotion of social housing during the XX century: although most of this heritage has become private, the archives are still available.

The research concerned different catalogues in Florence (*Archivio Ater/Casa SPA, Archivio Storico del Comune di Firenze, Archivio delle Ferrovie dello Stato*) and has identified a relevant number of projects of residential buildings. For each project, the definitive design related by technical specifications and quantity surveying of materials has been researched. The level of information is heterogeneous and not always the same, depending by catalogue, the contractor society, the years of constructions, the specific intervention.

In Table 1 an overview of the researched archives is shown. The documentation is listed within the different archives, describing the collected information in terms of textual and drawing contents. They are divided between the main structural elements composing a building: foundations (F), walls (W) and slabs/roofs (S). Later, the identified buildings were localized on the map of the city (Fig. 2). Contextually to this phase the CAD planimetries of each project have been reproduced. The final database is characterized by more than 300 URM buildings, realized through 143 planimetries, as several structures have been realized adopting the same design. A classification of the database within different architectural and structural features is presented in Ref. [35].

2.1. Building taxonomy: evidence from the research

The archive research allowed a technical characterisation of the investigated Public Housing interventions, and more in general, of the modern masonry residential stock settled in Florence. A preliminary vulnerability assessment of these buildings was investigated adopting the GNDT second level sheets [36]. The outcomes of this work showed a significant homogeneity within these structures, pointing out the inability of the empirical methodology, requiring analytical assessments [35]. Considering the obtained database, the most part of the buildings have the ground floor detached from the soil level (90.67%). Within them, the 42.16% of the stock, is characterized by the presence of a ventilation floor under the soil level (A-type), while the 48.50% has underground cellars (B-Type). Only 9.33% of the database does not have the ground floor, with the structure directly located over the ground (C-Type) (Fig. 3). Regarding the regularity/irregularity of the structures, the buildings are not characterized by vertical irregularities, as they present the same plans along the height with coherent reductions of both thickness of the bearing walls and involved masses. On the other side, they can show planar irregularities due to the combination of regular structures. An overview of the structural components of the building is proposed in the following sections.

Foundations. These investigated buildings present linear continuous foundations. Materially, they were realized through masonry foundations, concrete/inert-materials foundations. In minor cases, they can be realized by RC structures. In this research, several foundations realized with constipated concrete have been found. The excavation dimension was about 50–60 cm under the ground for the larger bearing structures. Following the classic scheme, they are usually 20–30 cm larger than the superior walls. In the case of RC foundation, some rectangular basement around 150 cm has been found.

Bearing walls. The bearing walls present common rules, where the technical system follows ancient and proven schemes. The investigated buildings present good empirical treatments. The masonry panels have structural continuity, and the masses are coherently distributed along the height. The perimetral walls of the lower levels are usually realized by rubble stone masonries; at the upper floor the thickness of the walls decreases, and they are generally realized by artificial materials. The rubble stone panels are composed by irregular stone elements joint with hydraulic mortar; in some cases, they are enriched by courses of clay bricks 1 m spaced. Specific attention to the corner connection may be found. At the latest floors the solid clay bricks can be substituted with

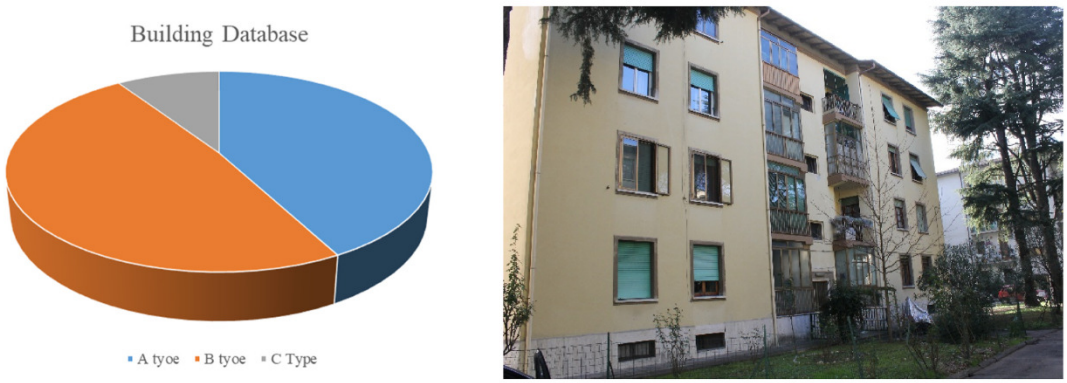

Fig. 3. On the left: classification of the database from the relationship of the building levels with the soil. On the right: an example of public house with underground cellars.

hollow masonry typologies. In Fig. 4 the level of detail of some technical documentation is presented.

Regarding the variability of the wall's thickness along the height, the 52.7% of the buildings has the perimetral walls with a variable thickness, while the 47.3% have a constant thickness. These data are related with the total height of the structures. Low buildings, ranging between one and two floors usually present a constant thickness of the bearing walls. On the other hand, buildings with three, four or more floors tend to have recesses in the thickness of the walls. The database counts the 36.7% of the buildings as A-Type, 53.1% for B-Type and 10.2% for C-Type. Concerning the thickness of the walls, the 57.9% has a variable thickness with the bearing structures characterized by recesses, only the 42.1% is made of constant buildings. In Table 2 a brief resume of the characteristics of the investigated buildings is shown.

Slabs. The floors are realized through RC joists alternated with hollow clay elements, topped by a concrete slab (max 4-cm of thickness). This represents a common technology for slabs in Italy, the so-called *solai in latero-cemento* which corresponds to mixed slabs. The thickness of the structural part is around 16/20 cm. In the first configurations the beams were reinforced only by the presence of a steel bar in the inferior part, later, 3 bars per beam were usually designed. The connection between the slabs and the bearing walls is guaranteed by the presence of RC ring beams all over the main structures. Concerning the bars, the documentation is scarce. When it has been found, it showed the presence of 4 bars φ14 in the perimetral ring beam; moreover, φ14 and φ10 were usually used for the reinforce of the slabs. The brackets had a dimension of φ6/20–30 cm. Concerning the ceilings, they are used for crawl spaces where there are not live loads. Sometimes they are realized with the same technology but lower thickness (12/16 cm), otherwise they are composed by steel beams alternated to hollow tiles generally without concrete slab.

Roofs. Roofs are generally made through wooden beams covered by wooden planks and roof tiles; sometimes, they are composed by prefabricated RC joists (Varese joists or similar), hollow tiles and finally hollow roof tiles. Normally, the crawl space has the concrete kerb over the perimeter of the building, and it is joined with the level floor, while the roof structure is not linked with the concrete ring.

2.1.1. Mechanical properties of the materials

The cognitive research allowed the identification of the geometries of the buildings as the definition of their structural characteristics. This section presents and discusses the mechanical properties of the materials adopted in the investigated buildings.

Masonry. Five different masonry typologies have been assumed for the bearing walls of the XX century buildings in Florence: chaotic rubble stone masonry RS, clay bricks and lime mortar CB, quasi-full bricks with cement mortar QB, concrete or clay blocks CC, semi-hollow concrete blocks HB. Concerning their mechanical properties, the starting point of the research was based on the data provided by the Italian code [37]. Then, a site-specific implementation of the mechanical values was made through a Bayesian approach, recently implemented in the National code. The Bayesian updating allows the improvement of the starting values, based on the implementation of new samples over a prior distribution [38,39]. In this work, the prior values were assumed on the distribution proposed by the technical legislation [37] for the different masonry typologies considered in the work. Then, the values have been updated assuming the experimental results presented in the Tuscan Masonry Database (TMDB) [40]. The latter contains a wide number of experimental tests performed in the Tuscany Region during the last decades by different research institutions. The mechanical values for the implementation have been selected between the tests performed over wall panels made during the XX century for the same masonry typologies. Data of experimental campaigns have been found for all the masonry types considered except the HB masonry, for which the code values have been adopted. Complexly, 27 compressive diagonal (CD) tests, 11 double flat-jack (DJF) tests, and 2 compressive (C) tests have been used. CD tests provide information about the Shear Modulus G and the shear strength τ_0. DJF and C tests provide results for the Elastic Modulus E and for the compressive strength f_m. An example regarding the update of the mechanical properties of RS masonry is presented in Table 3. Fig. 5 shows a comparison for the four investigated parameters, between the prior and the updated values. The final values have been taken considering both updates of each parameter as the physical relationships between them. The results present some differences between them. In some case, the updated values are lower than the

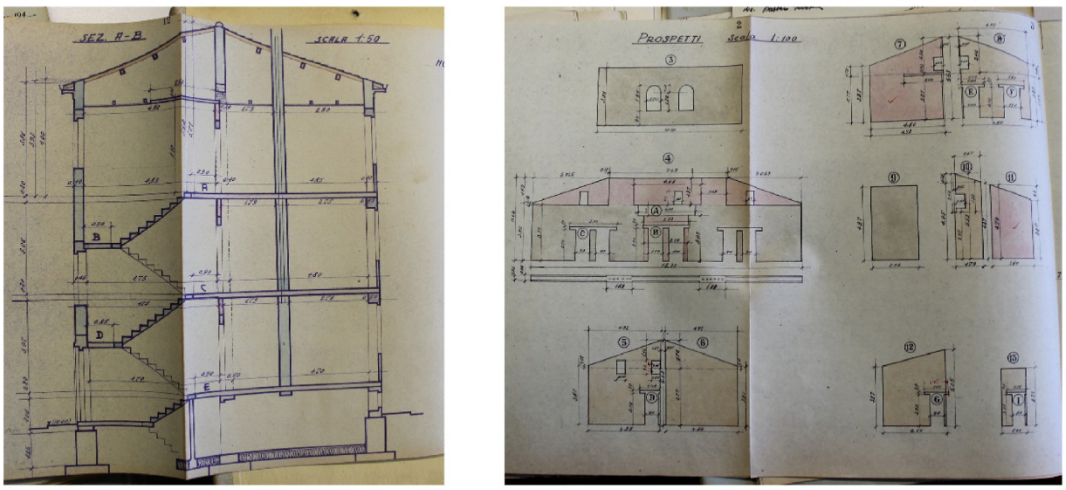

Fig. 4. Drawings from RFI Archive, details of masonry structures.

Table 2
Building features; ventilation floor and thickness of the bearing walls.

	A-type	B-type	C-type	Variable	Constant
Database	36.7%	53.1%	10.2%	57.9%	42.1%
3 storeys	54.8%	26.2%	19.0%	50.00%	50.00%
4 storeys	23.1%	75.8%	1.1%	78.8%	21.2%

Table 3
Rubble stone masonry, Bayesian approach. The number of the different tests (MP062, CD005) are referred to the names coded in the TMDB.

			f_m (MPa)	cov	τ_0 (MPa)	cov	E (MPa)	cov	G (MPa)	cov
Chaotic rubble stone masonry	*prio*	MIT2019	1.5	0.33	0.025	0.28	870	0.21	290	0.21
	DJF	MP062					2174			
	CD	CD005			0.025				284	
		CD006			0.038				232	
		CD007			0.032				338	
		CD008			0.036				106	
		CD009			0.022				43	
		CD014			0.03				566	
		CD015			0.039				360	
		CD016			0.031					
		CD017			0.044				629	
		CD018			0.024					
		CD019			0.023					
		CD020			0.023					
		CD021			0.069				407	
		CD028			0.042					
		CD029			0.058				1236	
		CD030			0.023				933	
		CD031			0.041				267	
		CD037			0.025				272	
		CD050			0.023					
	C	C109	1.04				322			
		C110					456			
	mean		1.04		0.03411		984		436.385	
	updated		1.270	0.278	0.034	0.203	970.47	0.158	421.24	0.165
			1.270	0.278	0.034	0.203	1263.72	0.165	421.24	0.165

mean values provided by the code. Nevertheless, the adopted mean values usually remain in the range of the prior distribution. The obtained upgrade is specifically referred for the Tuscan context, switching from general data valid for the entire Italian territory to site-specific results.

Concrete. For the concrete material, several studies have been conducted for the Tuscany Region [41]. A relevant quantity of samples has been extracted from public civil buildings; Cristofaro et al. [42] presented the mean values and the relative standard deviation for concrete classes depending on different decades of the last century. A minimum, mean and maximum value for the cubic compressive strength Rc, mean have been considered, from these parameters. Hence, three different values equal to 13.25, 21.18, and 30.92 MPa have been adopted.

Steel. In this work, the steel elements are only referred to the bars into the reinforced concrete. At the time, the steel bars were smooth reinforcing bars, characterized by the absence of shaped ridge structures. The mechanical properties were assumed based on the publications from the Campania Region [43]. Herein, a common steel material characterized by an Elastic Young's Modulus of 206 000 MPa and a characteristic yielding stress f_{ym} of 350 MPa was assumed.

3. Analytical assessment of a case-study

3.1. The case study

Inside the building database, a specific case study has been finally selected for an analytical assessment. It has been chosen within the simple block buildings. This typology represents the simplest and the more recurrent one. Several building plans have been found (Fig. 6). The simple block type is a standard typology for many cities of the Italian and European contexts. In fact, it has been used both in linear aggregation along the streets, both in isolated shapes. Concerning the structural disposition of the masonry walls, the buildings may have different configurations; the main one is obtained considering the façades and the side walls. The side walls are characterized by massive bearing walls with few openings due to the possibility of aggregation along the X direction. The façades are instead more divided between piers and spandrels.

The selected case study (Fig. 7) is a real case-study building located in the Novoli district, in the western part of the city. Due to its characteristics, the building represents a reliable benchmark representative of the building class. The construction was part of a parceling plan realized during the 50's. In the area where the building is settled, 18 different constructions were realized, adopting 11

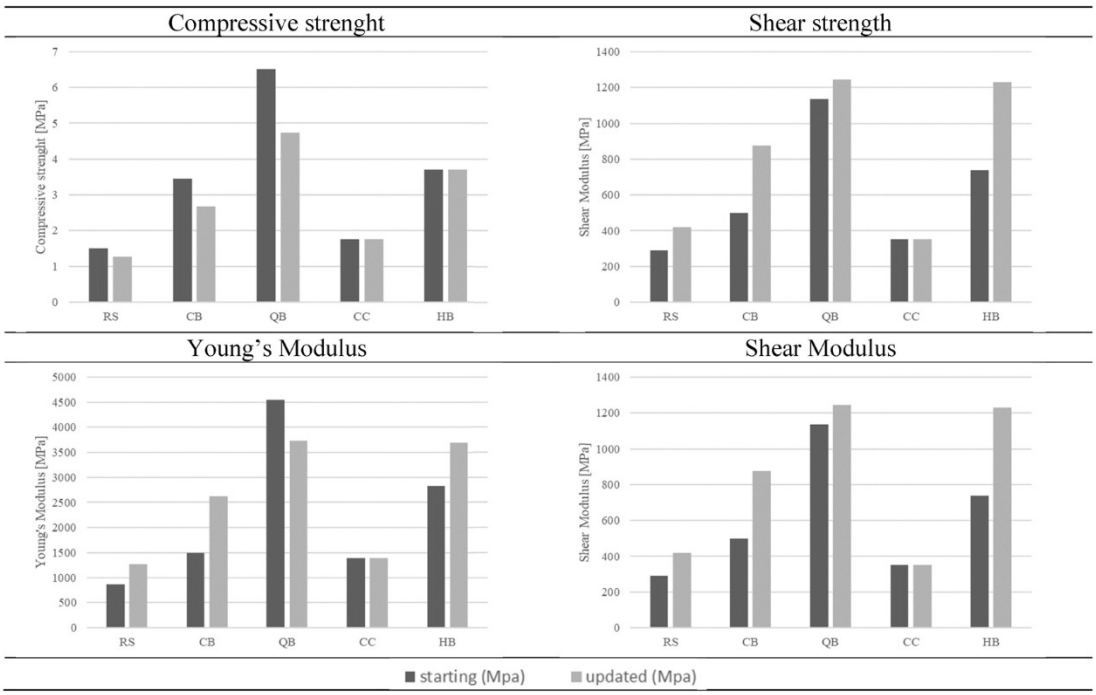

Fig. 5. Prior and updated distribution for the different mechanical parameters investigated.

different planimetries [21]. The design was used to realize two distinct constructions.

The house is a block-case building, constituted by four levels plus the basement level generating the ventilation floor. The construction has been selected on the basis of several features. Considering the empirical vulnerability assessment developed in Ref. [35], the vulnerability index of the building was close to the mean value of the database. Secondly, its ratio between the two geometrical sides, X and Y, is really close to the mean value of the ratio between the two geometrical sides of the total building database. Coherently with most of the investigated structures, the bearing walls present a decrease in their thickness along with the building height. Looking at the plan, the resistant wall disposition tends to highlight the characteristics pointed out in the previous section, showing a clear distinction between the façades and the side walls. In the internal part, the walls oriented in the Y direction are mostly solid walls with few openings. Since the walls and the slabs are orientated along both directions, the internal bearing wall's disposition can be also partially considered as a mixed one.

3.2. Structural modeling

In this work, an Equivalent frame model (EFM) has been realized. EF approaches have been widely validated by experimental and post-earthquake damage observations. The definition of the EFM was done through the software Tremuri [44,45]; the masonry is modelled as a nonlinear beam element with six degrees of freedom and a constitutive model with a resistance limit. A multilinear constitutive law based on a phenomenological approach and characterized by both, a monotonic and a cyclic response is assumed [46]. It considers a bilinear relation with a cut-off in strength and stiffness decay in the nonlinear phase. The elastic branch is given by the initial stiffness, which is computed starting from a cracked configuration (50% of reduction) as recommended in the Italian codes; then, a secant stiffness representing the progressive degradation of the material is assumed. The constitutive law allows to describe the nonlinear response defining damage levels DLs that correspond to the strength degradations [47]. The values of the drift levels and the strength decays have been taken from other works and experimental campaigns presented in literature [48–51]. The software implements three different failure criteria, i.e., flexural rocking, shear sliding and diagonal-cracking; the nonlinear behaviour is activated when the first criterium achieves his threshold value. The ultimate bending moment is based on a no-traction material where a nonlinear reallocation of the stress is performed (rectangular stress-block) [4]. For the shear, the Turnsek and Cacovic criterion is assumed, aimed to interpret the diagonal shear failure mode [52].

In addition, the drift is taken into account in order to control the ductility of the elements. The internal stresses are redistributed in order to maintain the equilibrium, while the elements that reach their ultimate drift are deleted from the calculation.

In the structural modeling, the ring beams at the slab levels have been considered coupled at the masonry spandrels generating a strut-and-tie mechanism, where the maximum compression value in the spandrels is assumed equal to the tension strength in the coupled elements [51]. In this work the RC tie beams have been assumed equal to their full length, however this aspect can be further investigated as pointed out in different works [53,54].

The diaphragms are modelled as rigid membranes distributing the seismic actions in the perimetral nodes. Tremuri models the slabs as orthotropic membrane elements characterized by different Elastic Moduli $E_{1,2}$ and the equivalent shear modulus G. In this work, the

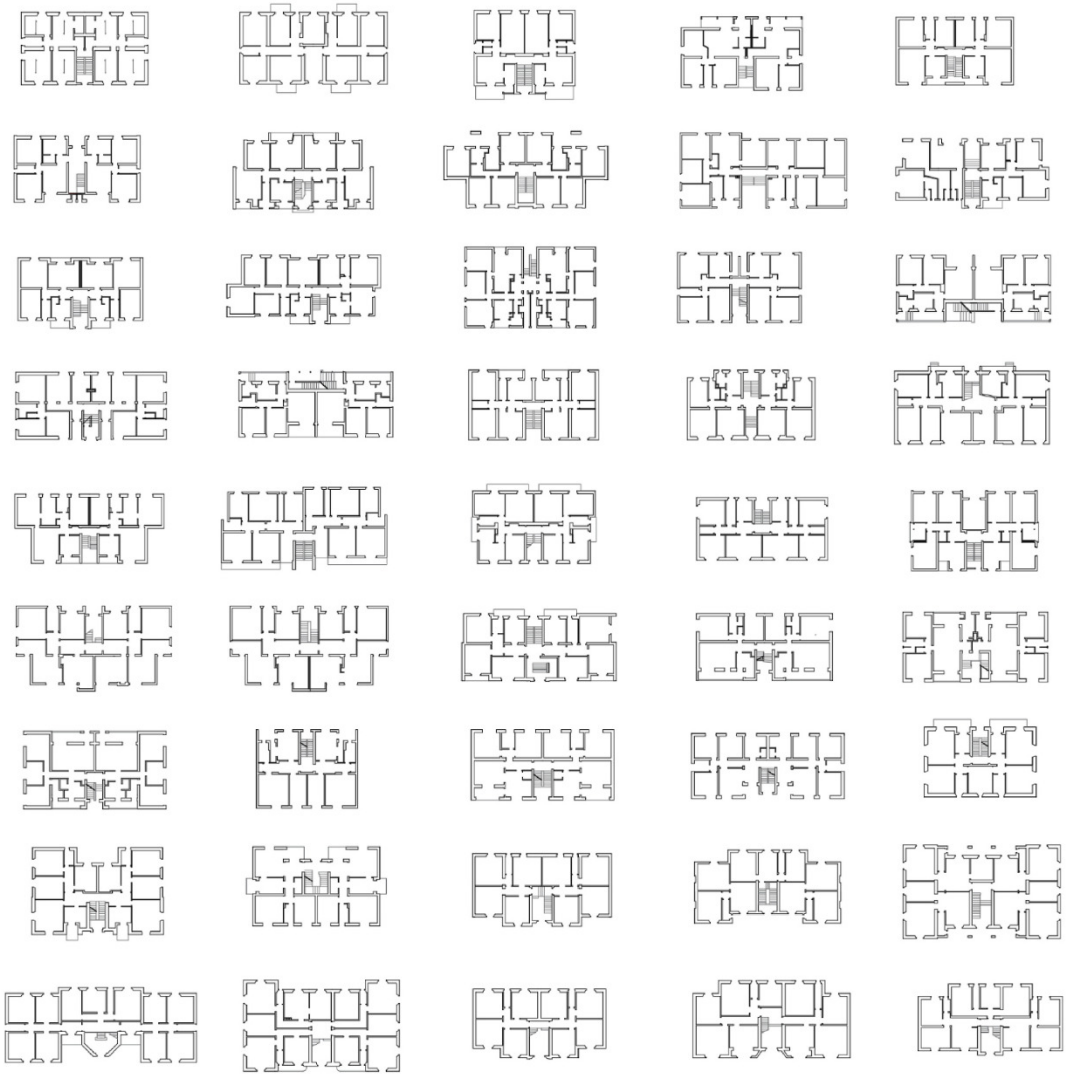

Fig. 6. Building planimetries of the found block-case buildings.

RC membranes topped with the reinforced slab have been assumed as rigid diaphragms. The execution of an ambient vibration test performed over two case studies confirmed the reliability of the rigid slabs, as other contributions presented in literature [55–57].

4. Probabilistic framework

A probabilistic framework based on nonlinear static analysis (NLSA) has been defined. In the procedure, both aleatory and epistemic uncertainties have been considered. The aleatory uncertainties have been modelled as continuous random variables, and the epistemic ones have been modelled through a logic tree approach; hence, the results of both components have been investigated in terms of sensitivity analysis. The vulnerability assessment of the case study has been expressed in terms of probabilistic fragility curves. A flowchart of the procedure followed is shown in Fig. 8. The definition of fragility curves allows the definition of the probability of occurrence of a certain damage level as a function of the intensity measure of the ground motion [58]. Different fragility curves have been developed in the last years through several different contributions [12,14]. Within the different approaches developed in literature, the analytical ones are derived from the static or dynamic analysis of structural models [59–61]. At the basis of the derivation of fragility functions, two parameters are necessary: the Intensity Measure and the Dispersion. Given a value *im* of the Intensity Measure (*IM*), the fragility function expresses the probability that a Limit State (LS) is reached:

$$p_{ls}(im) : P\,(\,d > D_{LS}\,|im\,) = P\,(im_{LS} < im\,) = \Phi\left(\frac{\log\frac{im}{IM_{LS}}}{\beta_{LS}}\right) \tag{1}$$

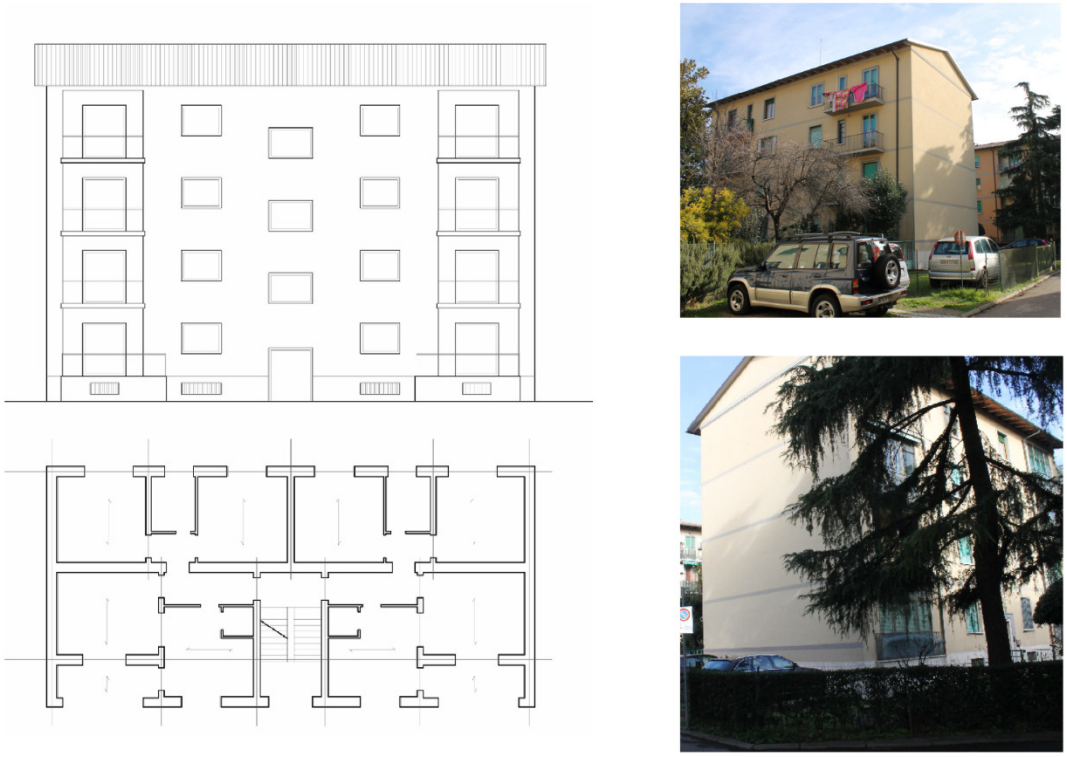

Fig. 7. The selected case-study; building drawings and photos from the exterior.

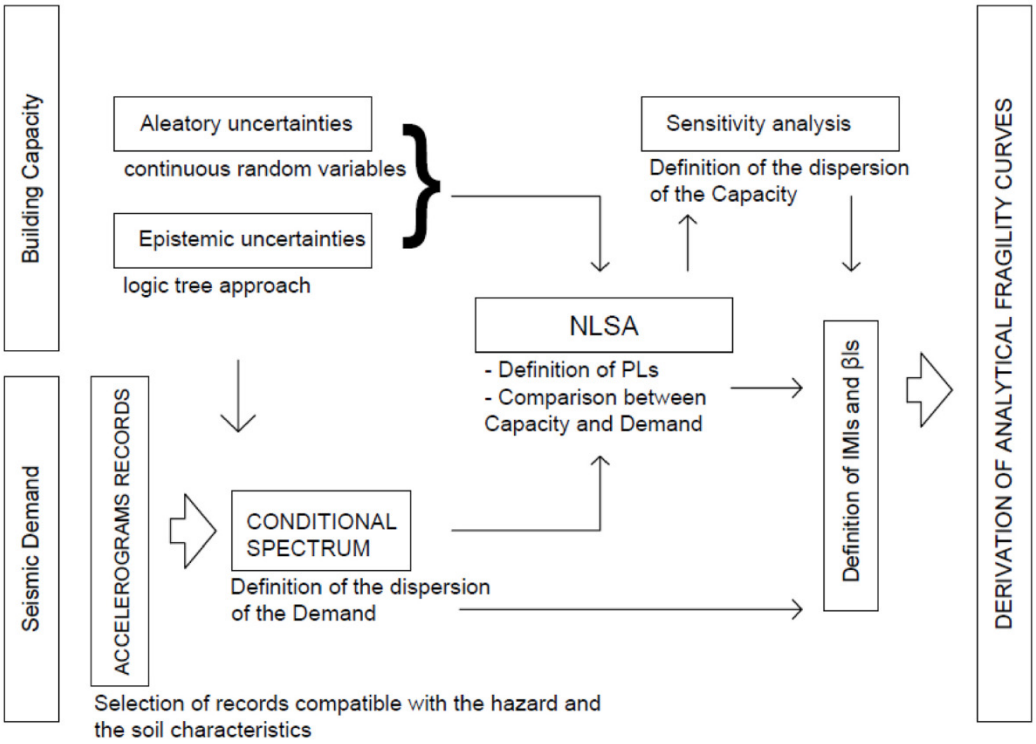

Fig. 8. Flowchart of the analytical assessment.

where d is the displacement considered for the assessment of seismic behaviour, DLs is the Limit State Treshold, IM_{LS} is the median value of the lognormal distribution of the intensity measure im_{LS} that reaches the LS threshold and β is the total standard dispersion.

NLSAs have been chosen as assessment method. Two different load patterns, one proportional to the masses of the building and one to the inverse triangular pattern have been used, separately, according the two different examined directions. Then, the assessment of the seismic capacity has been done defining the performance levels (PLs) - *DL1* slight damage, *DL2* moderate, *DL3* heavy, *DL4* very heavy, *DL5* collapse - on the pushover curves. Each LS has been defined according to a multiscale approach, considering three different scales of interest: global, macroelement, element [62]. The attainment of each PL is achieved when for the minimum performance point on the pushover curve according to the three aforementioned criteria (please see the supplementary material).

To define the PL able to attain a certain DL, the Intensity Measure IM to express the PL is needed. Numerous IMs exist in literature [63]; in this work referring to the URM buildings, the peak ground acceleration PGA has been adopted. Its reliability towards the investigated structures has been proved by different authors as masonry buildings are characterized by short fundamental periods [64–67]. To compare the seismic capacity with the site demand the Capacity Spectrum Method CSM [68] with over-damped spectrum has been used. The latter has been preferred to the N2 method [69] in accordance with the PERPETUATE guidelines and other contributions which pointed its reliability especially in case of irregular structures [62,70]. In the approach the overdamped spectra are defined according to the damping correction factor η, which is defined as a function of the equivalent viscous damping ξ_{eq}, accounted as the sum of the elastic viscous and hysteretic contributions $\xi_{eq} = \xi_{el} + \xi_{visc}$. In the presented work the elastic viscous damping has been considered equal to 5%, while the hysteretic damping has been analytically calculated performing cyclic pushover analysis. The cyclic pushover analyses have been executed in displacement-control over the mean models considered in the probabilistic assessment. More details about the adopted procedure can be found in Ref. [51].

To define the fragility curves, the definition of the dispersion is needed. In this work, the two sources of uncertainties (*i.e.* the uncertainties in the seismic demand β_D and the seismic capacity β_C) have been assumed and considered as statistically independent.

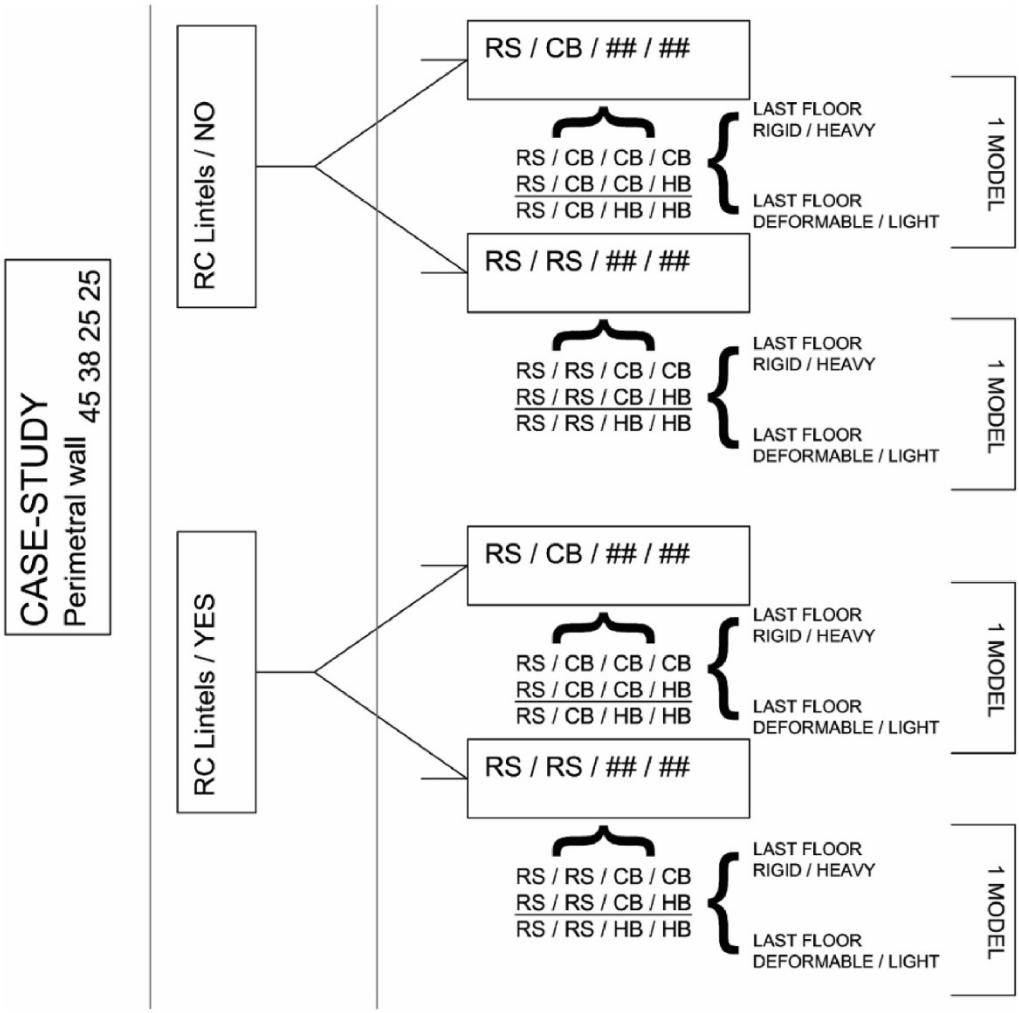

Fig. 9. The logic tree approach adopted in this work.

The final computation of the uncertainty of the model is given by:

$$\beta_{tot,DL} = \sqrt{\beta_{D,DL}^2 + \beta_{C,\ DL}^2} \tag{2}$$

For the Seismic Capacity, the uncertainty propagation has been assessed through the Response Surface Method [71]. The aleatory uncertainties have been considered through a simplified procedure defined as the star design with central star approach. Its adoption is characterized by the performance of $2\,N + 1$ analyses, where N represents the number of variables [51,54]. For the seismic hazard, the seismic demand has been considered for a referred Return Period considering the soil spectrum defined by the Italian code (soil B, return period 475 years).

According to the CNR-DT212 recommendations [72], a sample of 30 accelerograms compatible with the selected spectrum has been considered. In this work the data obtained by the Italian databases of INGV have been used. The selection of the compatible records was conducted using the software Rexel [73] adopting the European strong motion database (http://esm.mi.ingv.it) for the ground motion selection [74]. Complexly, a set of 30 accelerograms compatible with the area of interest have been set. The spectra have been considered by the geometrical mean between the two planar directions; hence, the median spectrum has been then conditioned by the fundamental mode of the building models, computed by linear dynamic analysis. The uncertainty in the spectral shape is given by calculating the median spectra over a sample of 30 soil-compatible ground motions. The median spectrum represents the 50% fractile of the sample. The uncertainty is finally given considering the 16th and 84th fractile response spectra of the selected time histories $0.5(\log PGA_{D,84} - \log PGA_{D,16})$.

4.1. Epistemic uncertainties and logic tree model

Within the selected case study, several uncertainties can still be considered, especially regarding the material characteristics of the bearing walls at the different levels. This lack of knowledge was modelled through a logic tree approach, where the different logic tree branches have been assumed statistically independent. A scheme of the developed logic tree is presented in Fig. 9. Considering the evidence of the investigation phase of this work, the first differentiation is obtained, distinguishing the models according to the eventual presence of lintels over the openings. RC elements over the openings leads to a clearer shear-type model, where the spandrels couple the piers within the openings. Then, two other different classes have been gathered. The structures have been considered with a thickness reduction of the bearing walls along the heights. Four different thicknesses of the masonry walls, based on the drawing of the structure, have been assigned. The bearing walls are characterized by 45 cm thickness at the ground level, 38 cm at the first level and 25 cm at the upper floors. RS, CB, and HB masonries been considered for the bearing structures. QB masonry has been adopted for the partition walls. Preliminary to the final proposed classification different combinations have been studied. The RS masonry was accounted at the ground level and at the first floor. The CB masonry was proposed both at the first, the second and the third floor. Finally, the HB masonry was considered at the last two levels. Assuming hierarchical roles within the typologies (e.g., the HB masonry is always adopted over the CB masonry and never under it) six different models have been obtained. The models have been firstly grouped considering the differentiation proposed at the first level, where RS or CB masonry was proposed. In fact, the results of the pushover curves showed that the variability of the second floor represented the core of the response variations.

The pushover responses pointed out a low sensitivity of these different assumptions to the seismic performance of the structural models, so the logic tree has been simplified considering just one model representative of the three different configurations. A final uncertainty was given by the ceiling characteristics. Two different configurations for the ceiling have been accounted, one adopting a rigid and heavy slab (RH) and the other assuming a light and deformable membrane (LD). The results in terms of global response showed the low sensitivity of the pushover for the considered aspect, therefore only one model was adopted (LD models). Regarding the roof, it has been only considered in terms of masses and distributed weights. In Table 4 a resume of the considered structural properties of slabs and roofs are shown. Finally, four structural models have been assumed as representative of the possible obtainable structural configurations of the case-study.

Nonlinear static analyses have been performed to assess the influence of the different logic tree branches. The results in terms of pushover curves are shown in Fig. 10. The plotted pushover curves assume the displacement d normalized to the total height h of the model in abscissa (d/h), while in ordinate it plots the base shear V normalized over the total weight of the building, W (V/W).

Comparing the four models, the lintels contribution in the coupling role between the different piers can be noted, mainly in X direction, where several openings characterize the bearing walls. In this direction, the models without lintels present a lower elastic stiffness and a more pronounced ductility. The presence of spandrels over the openings defines a more evident coupling between the piers, anticipating their crisis because of the shear actions. The mass proportional pattern always presents a higher stiffness slope and generally, a higher maximum value of the base shear too. On the contrary, the inverse triangular shows a lower stiffness and lower maximum base shear values. Still, it allows a major contribution in the plastic phase, leading to wider plasticization of the elements

Table 4
Structural characteristics of slabs and roofs in the analysis.

	Rigid/heavy case		Light/deformable case	
L1-2-3	Structural: 2.45 kN/m^2 Non-structural: 1.00 kN/m^2	Infinitive stiffness	Structural: 2.45 kN/m^2 Non-structural: 1.00 kN/m^2	Infinitive stiffness
L4	Structural: 2.45 kN/m^2 Non-structural: 1.00 kN/m^2	Infinitive stiffness	Structural: 0.2 kN/m^2 Non-structural: 0.5 kN/m^2	G: 11666.67 MPa
Roof	Non-structural: 1.10 kN/m^2	Loads only	Non-structural: 1.10 kN/m^2	Loads only

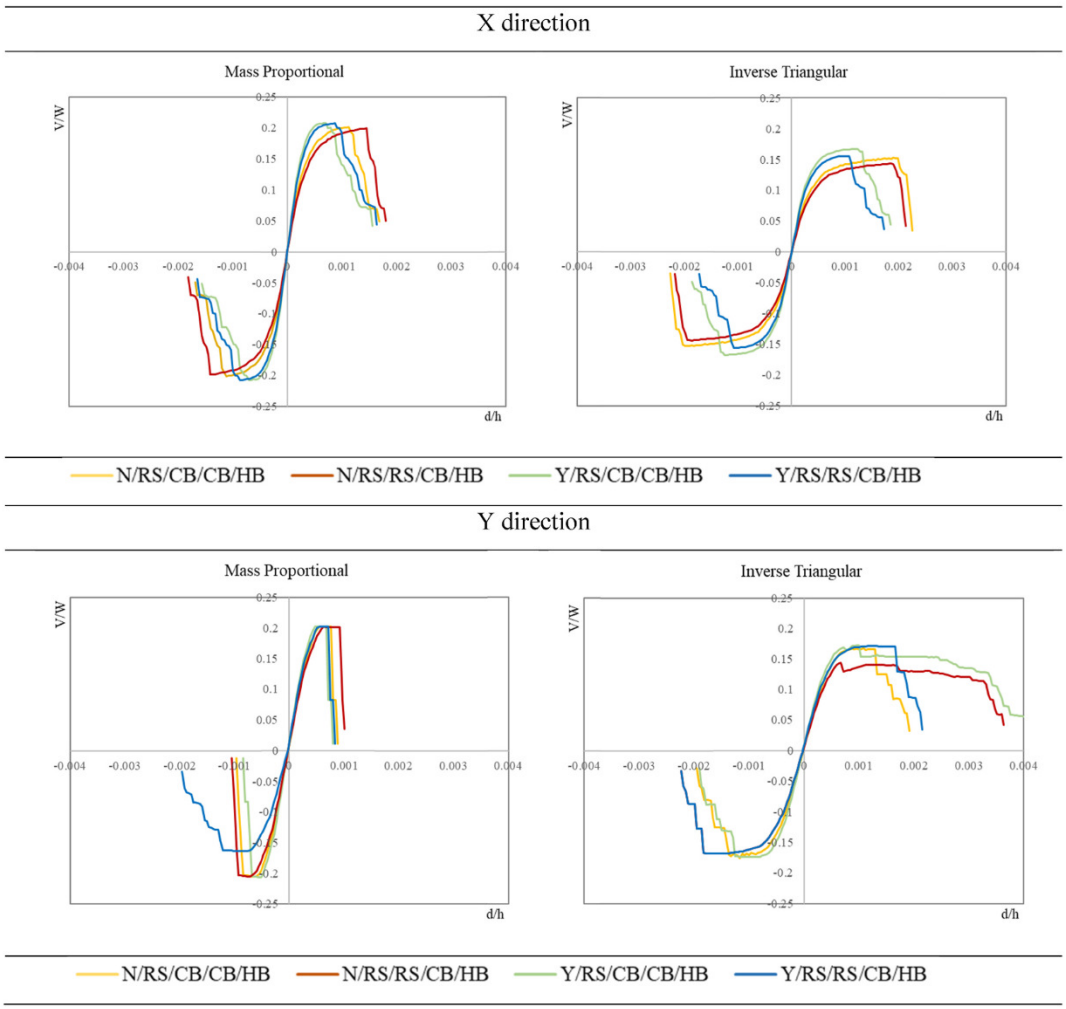

Fig. 10. Pushover curves of the No-lintels and Yes-lintels models according to the two directions and the two load patterns.

before the collapse. This can be mostly asserted by looking at the damage patterns and the failure mechanisms of the structural models. Complexly, all the models exhibit the same failure patterns, *i.e.* the shear failure of piers at the ground level, with both seismic distributions. The inverse triangular pattern allows a more distributed damage along the façades, stressing the lower and the upper part differently. For the structural configuration of the case study, the inverse proportional pattern leads to lower base shear values, nonetheless, it points out a bigger nonlinear ductility. On the other side, the mass proportional pattern seems to be more demanding in the plastic phase, quickly increasing damage degradation in the piers of the ground floor.

The different behaviour of the models towards the load patterns along the two main directions can be justified by the different distribution – firstly – of the resistant walls - and secondly – by their masonry discretization. In the *Y* direction, the predominant behavior of the structure can be associated with a frame-behaviour. In contrast, in the *X* direction the façades tend the structure to the perfect idealization of the frame structure.

4.2. Aleatory uncertainties and sensitivity analysis

For each of the four models previously described, 7 aleatory uncertainties have been considered. To this aim, the star design with a central point approach has been adopted. Assuming the $2\,N + 1$ analyses, with N is the number of aleatory uncertainties, 15 different models have been studied for each logic tree branch. 60 different models have been assessed by means of NLSAs. The aleatory variables considered in this paper are presented in Table 5. The first three variables, $X_{1,2,3}$ concern the mechanical properties of the resistant walls. The different mechanical properties of each material are considered as dependent parameters, so they varied together. The fourth variable, X_4, is represented by the uncertainties in the concrete. For the steel bars, a deterministic value has been adopted, without performing any sensitivity. Regarding the last three parameters, $X_{5,6,7}$ they are related to the properties of the nonlinear constitutive law adopted in the modeling. X_5 rules the degradation of the initial stiffness assumed for the masonry panels. Finally, X_6 and X_7 collect parameters that affect the plastic phase and the nonlinear degradation. The values of θ_p indicate the drift values associated to the progressing damage, for different failures, for combined compressive and bending stress or for shear, respectively; the

Table 5
Aleatory variables introduced in this work.

	Aleatory uncertainties		*min*	*mean*	*max*	
X_1	RS	*E (MPa)*	1054.9	1263.7	1472.4	Lognormal distrib
		G (MPa)	351.6	421.2	490.8	
		f_m *(MPa)*	0.916	1.27	1.623	
		τ_0 *(MPa)*	0.026	0.033	0.040	
X_2	CB	*E (MPa)*	2284.9	2625.1	2965.3	Lognormal distrib
		G (MPa)	761.6	875.0	988.4	
		f_m *(MPa)*	1.97	2.66	3.36	
		τ_0 *(MPa)*	0.049	0.082	0.114	
X_3	HB	*E (MPa)*	1200	1400	1600	Lognormal distrib
		G (MPa)	300	350	400	
		f_m *(MPa)*	1.50	1.75	2.00	
		τ_0 *(MPa)*	0.095	0.11	0.125	
X_4	concrete	*Rcmean (MPa)*	13.25	21.18	30.92	Deterministic
X_5	*kr*		0.5	0.65	0.8	Beta distrib
	kel		1.25	1.50	1.75	
X_6	*drift piers*	$\theta_{P,PF3}$	0.0046	0.006	0.0074	Beta distrib
		$\theta_{P,PF4}$	0.0078	0.01	0.0122	
		$\theta_{P,PF5}$	0.012	0.015	0.01796	
		$\beta_{PF,E3}$		1.00		
		$\beta_{PF,E4}$	0.8	0.85	0.9	
		$\theta_{P,S3}$	0.0023	0.003	0.0037	
		$\theta_{P,S4}$	0.0039	0.005	0.0061	
		$\theta_{P,S5}$	0.012	0.015	0.01796	
		$\beta_{S,E3}$	0.6	0.7	0.8	
		$\beta_{S,E4}$	0.25	0.4	0.55	
X_7	*drift spandrels*	$\theta_{S,3}$	0.0015	0.002	0.0025	Beta distrib
		$\theta_{S,4}$	0.0045	0.006	0.0075	
		$\theta_{S,5}$	0.015	0.020	0.025	
		$\beta_{PF,E3}$	0.3	0.500	0.7	
		$\beta_{PF,E4}$	0.3	0.500	0.7	

β values indicate the associated residual strength. Different values are considered for the piers and for the spandrels respectively. For these parameters, since the distribution ranges in a finite interval, the Beta distribution has been adopted [72]. The different pushover results have been firstly discussed in terms of capacity curves, then in terms of IM values for the LS attainments. The multiscale approach described in the probabilistic framework has been adopted. The results provided different results; nevertheless, in general, it is possible to point out a main prevalence of the *G* criterium for attaining the LSs. This can be mostly justified by the story failure of the buildings, which characterize a limited number of elements. In Fig. 11 the variations in the capacity curve due to the aleatory variables are presented for the model N_RS_CB_CB_HB. Finally, in this work, the comparison between the different models is obtained in terms of IM. The sensitivity of each parameter was accounted for in terms of comparisons between the PGA values needed for the attainment of

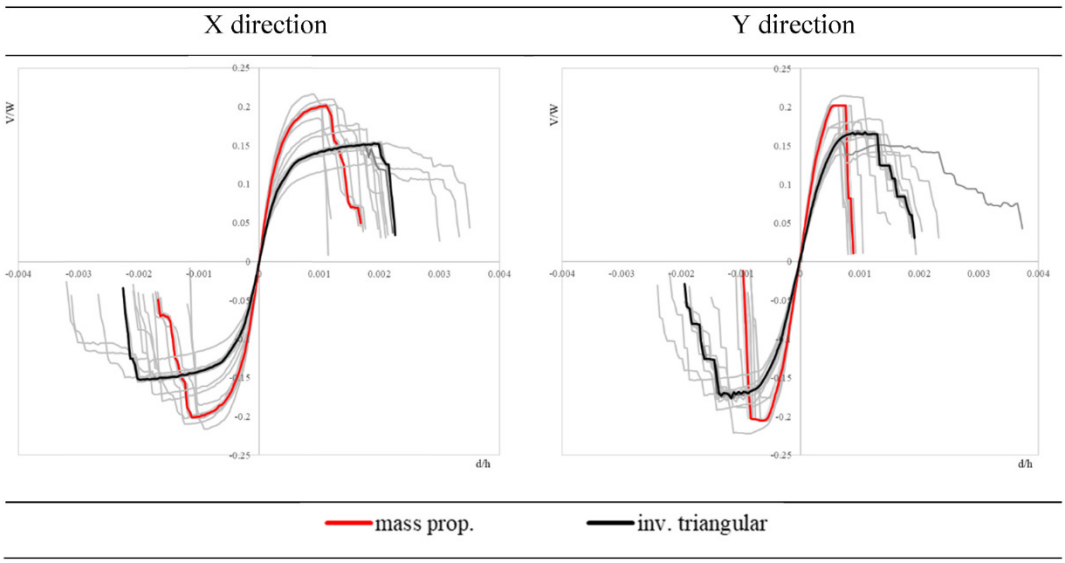

Fig. 11. Pushover curves for the N_RS_CB_CB_HB model according to the two directions and the two load patterns.

a certain DL.

The sensitivity of the different considered models has been studied considering the CNR-DT 212 [72] recommendations. The aleatory sensitivity of variables X_k is assessed through the variable $\Delta_{PLi,Xk}$ computed as:

$$\Delta_{PLi,\ Xk} = 2\,\frac{IM_{PLi,k-max} - IM_{PLi,k-min}}{IM_{PLi,k-max} + IM_{PLi,k-min}} \tag{3}$$

To consider the sensitivity of the epistemic uncertainties, given M branches, the j-th epistemic uncertainty is expressed through the $\Delta_{PLi,Yk}$ parameter, as:

$$\Delta_{PLi,\ Yj} = 2\,\frac{\max\left(u_{j,\ IM_{PLi},\ mean,q}\right) - \min\left(u_{j,\ IM_{PLi},\ mean,q}\right)}{\max\left(u_{j,\ IM_{PLi},\ mean,q}\right) + \min\left(u_{j,\ IM_{PLi},\ mean,q}\right)} \tag{4}$$

Where $\mu_{j,I\ MPLi,\ mean,q}$ is the mean of the different IM_{Pli} values outcoming from the logic tree approach by assuming the mean value for all the random variables. The sensitivity of each parameter can be assessed by the definition of sensitivity classes (SC). Three SCs are here defined: high sensitivity (SCH), medium sensitivity (SCM) and low sensitivity (SCL) [75]. The three classes are defined as a function of the $\Delta_{PLi,Xk}$ (or $\Delta_{PLi,Yk}$). SCH for $\Delta_{PLi,Xk}$ (or $\Delta_{PLi,Yk}$) $> 2/3\ \Delta_{PLi,\ max}$; SCM: $1/3\ \Delta_{PLi,\ max} \leq \Delta_{PLi,Xk}$ (or $\Delta_{PLi,Yk}$) $\leq 2/3\ \Delta_{PLi,\ max}$; SCL: $\Delta_{PLi,Xk}$ (or $\Delta_{PLi,Yk}$) $\leq 1/3\ \Delta_{PLi,\ max}$.

The results, in terms of PGA presents some deviation. Concerning the epistemic branches, the results of the sensitivity analysis showed a low sensitivity of the different models to the seismic response. On the other side, wider considerations may be done for the aleatory uncertainties. The aleatory variable X_1, X_2 and X_6 show higher sensitivity. Concerning X_1, 65% of the variables are scheduled into the SCH class, approximately equally distributed along with the different models and the different DLs, while 20% is given for SCM and the 15% for SCL. X_2 is divided as 56% for SCH, 23% for SCM and 21% for SCL. In this parameter, some difference is involved, especially for the higher DLs. In the case of no-lintel-models (N), the aleatory variable points out its sensitivity for the lower DLs, (*DL1* and *DL2*), while for the *DL3* and *DL4*, it is for the 53% of the times in SCL. On the other side, in case of yes-lintel-models (Y) the influence of the parameter is extremely sensitive especially for *DL4* (68.75% in SCH). The influence of X_3 does not seem so relevant. This is ascribable to the failure collapses of the models, which mostly regard the lowest floors. Yet, the influence of the concrete variability ranges between the SCL and the SCM, with a prevalence of SCL (74% of the parameters are in SCL). A higher interest is pointed out by the variable X_5 especially in the definition of the DL1. Concerning parameter X_6, it denounces a discrete sensitivity to the seismic response of the models. The 26.5% of the parameter enter in SCH class, with a 27.5% in SCM and the 46% in SCL, respectively. Despite the prevalence of the SCL class, this parameter mostly influences the performance of the models for the highest DLs. The sum of *DL3* and *DL4* it shows a SCH 26 out 32 times (81%). Finally, parameter X_7 shows a limited sensitivity. In Fig. 12 the results of the variability in terms of IM are shown for DL3.

4.3. Derivation of analytical fragility curves

Assumed the PGA values for the different DLs and the aleatory and epistemic models, fragility curves can be finally derived. The analytical formulation has been applied separately to the four models, according to the assumption of statistical independence of the different logic tree branches. To derive the fragility curves, the total dispersion β_T of the models needs to be computed. According to the described procedure, the adopted dispersion accounts for both contributions of the seismic demand and the building capacity. In Fig. 13 the PGA values and the relative dispersions for the no-lintel and yes-lintel models, respectively, are shown.

The plotted PGA values are referred to the minimum value between the positive and the negative contributions according to each seismic load pattern and each direction. The four models show some difference between the seismic performances of the structures. Specifically, the ductility capacity expressed in the X direction is highlighted by the bigger differences involving the PGA values for the attainment of the different *LSs*. In the Y direction, the variations are minor, with closer PGA values, especially between *DL3* and *DL4*. The vicinity of the *PLs* in the nonlinear phase confirm the trends already pointed out with the pushover curves. Concerning the dispersion values, β_T ranges between 0.1 and 0.22. It tends to increase along the development of the different *DLs*, especially in the X direction. The inverse triangular pattern is the one with the highest dispersions. Excluding those values, the dispersion rates are low, and they mostly range around 0.15.

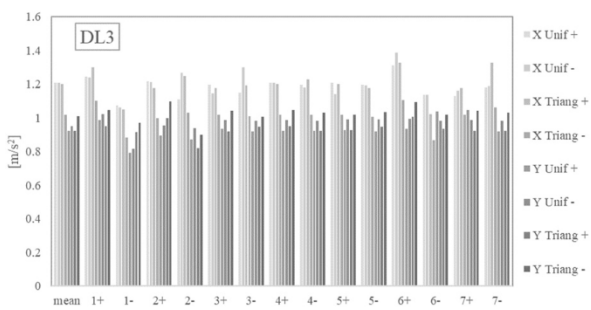

Fig. 12. Variability of the capacity response due to the aleatory uncertainties.

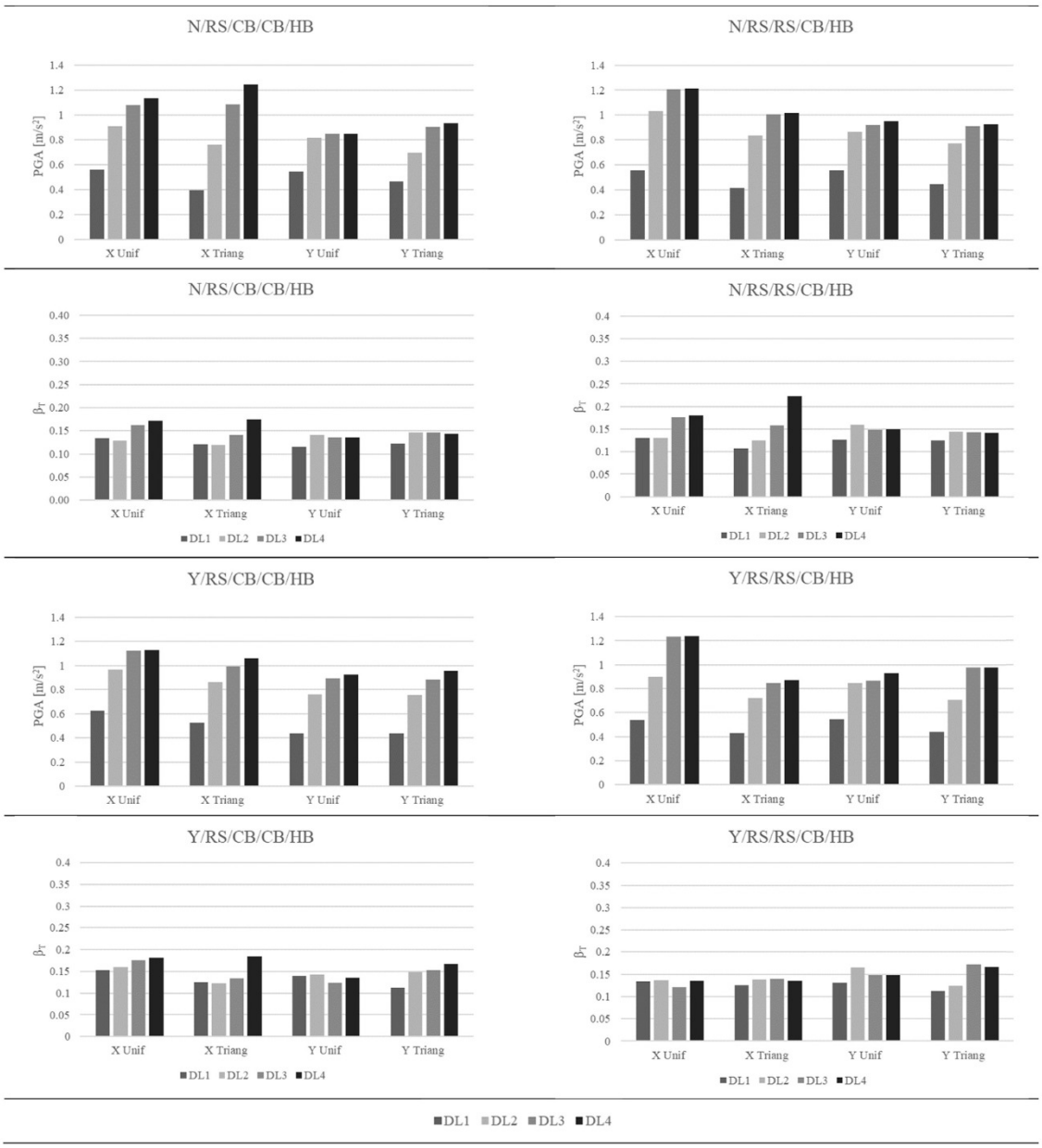

Fig. 13. The PGA values and the relative dispersions for the four models.

Finally, the analytical curves can be derived for each direction and each seismic load pattern. In Fig. 14 and Fig. 15 the plots are shown. Looking at the figures, the performance of the models points out some differences. Concerning both load patterns, for the two directions, usually, a higher offset distance insists between the *DL1* and *DL2*; then, the curves express a relative brittle behaviour with fast attainment of the further *LSs* and limited distances between *DL2*, *DL3* and *DL4*. This is pointed out by different models; in *X* direction, in models N/RS/RS/CB/HB Y/RS/CB/CB/HB, for the mass proportional pattern the fragility curves are plotted almost simultaneously. On the other side, the inverse triangular pattern generally exhibits a higher scatter between the two *LSs*, in all the models expect for Y/RS/RS/CB/HB. In the other cases, some superimposition between the two curves is pointed out, especially for low PGA intensities (models N/RS/RS/CB/HB and Y/RS/CB/CB/HB). This is justified by the different inclinations of the curves combined with the close distances of the PGA values for the attainment of the LSs and, because of the intrinsic definition of progressive *DLS*, it won't be considered in the definition of damage scenarios.

In the *Y* direction, the low ductility of these structures was already highlighted; the models show a relevant nearness between from *DL2* to *DL4*, which prove the rapid nonlinear degradation of the model. The mass proportional pattern leads to close fragility curves from *DL2* to *DL4*, especially for the two models without lintels.

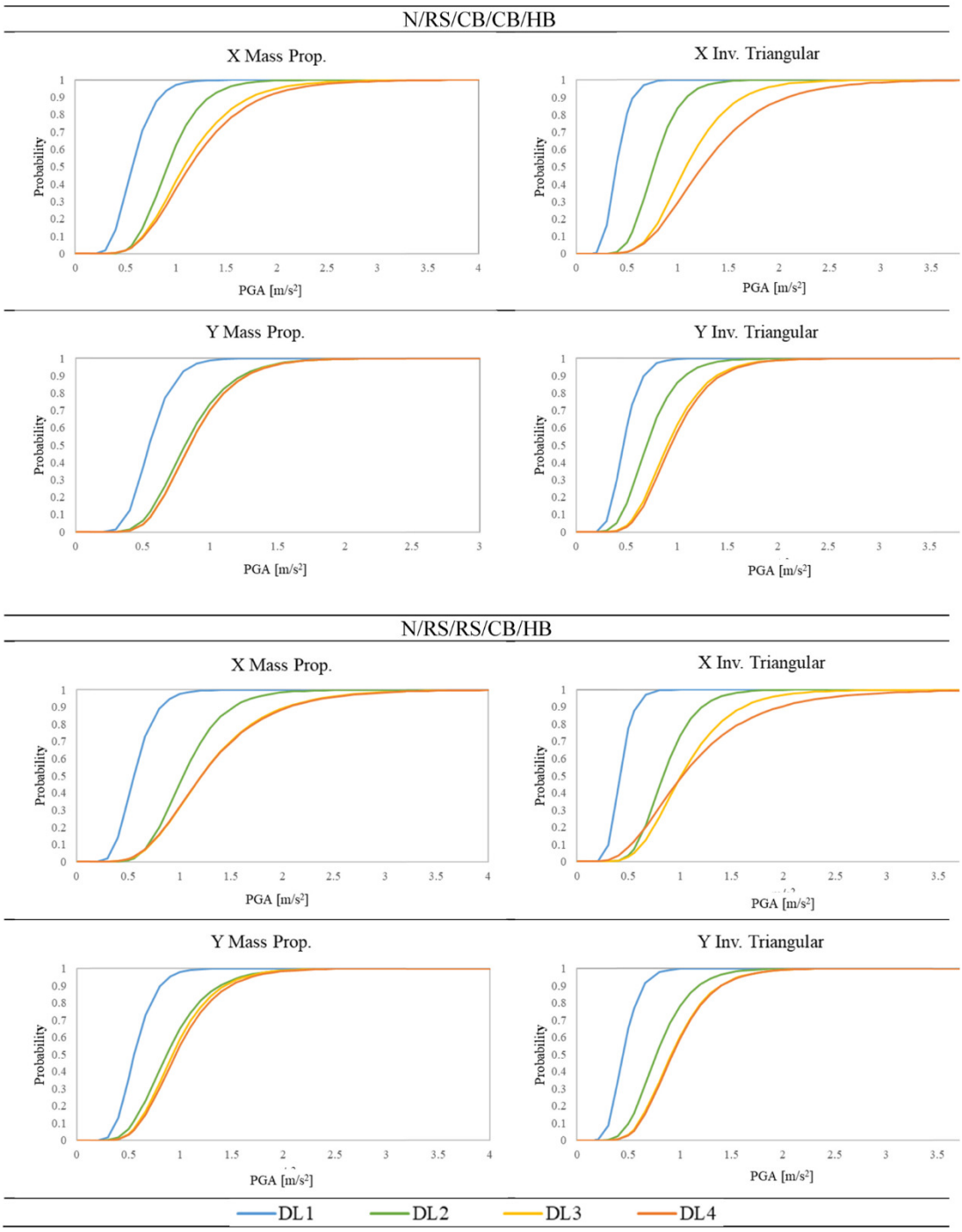

Fig. 14. The fragility curves for the two no-lintel models.

Once the fragility curves are derived, the damage state *DS* probability distribution can be obtained. These discrete probabilities have different formulations considering the k-th LS considered. For $LS_{k\ 1,2,3}$ they are expressed by:

$$p_{DSk}(im) = p_{LS\ k}(im) - p_{LS\ k+}(im) = \Phi\left(\frac{\log\frac{im}{IM_{LS\ k}}}{\beta_{LS\ k}}\right) - \Phi\left(\frac{\log\frac{im}{IM_{LS\ k+1}}}{\beta_{LS\ k+1}}\right) \tag{5}$$

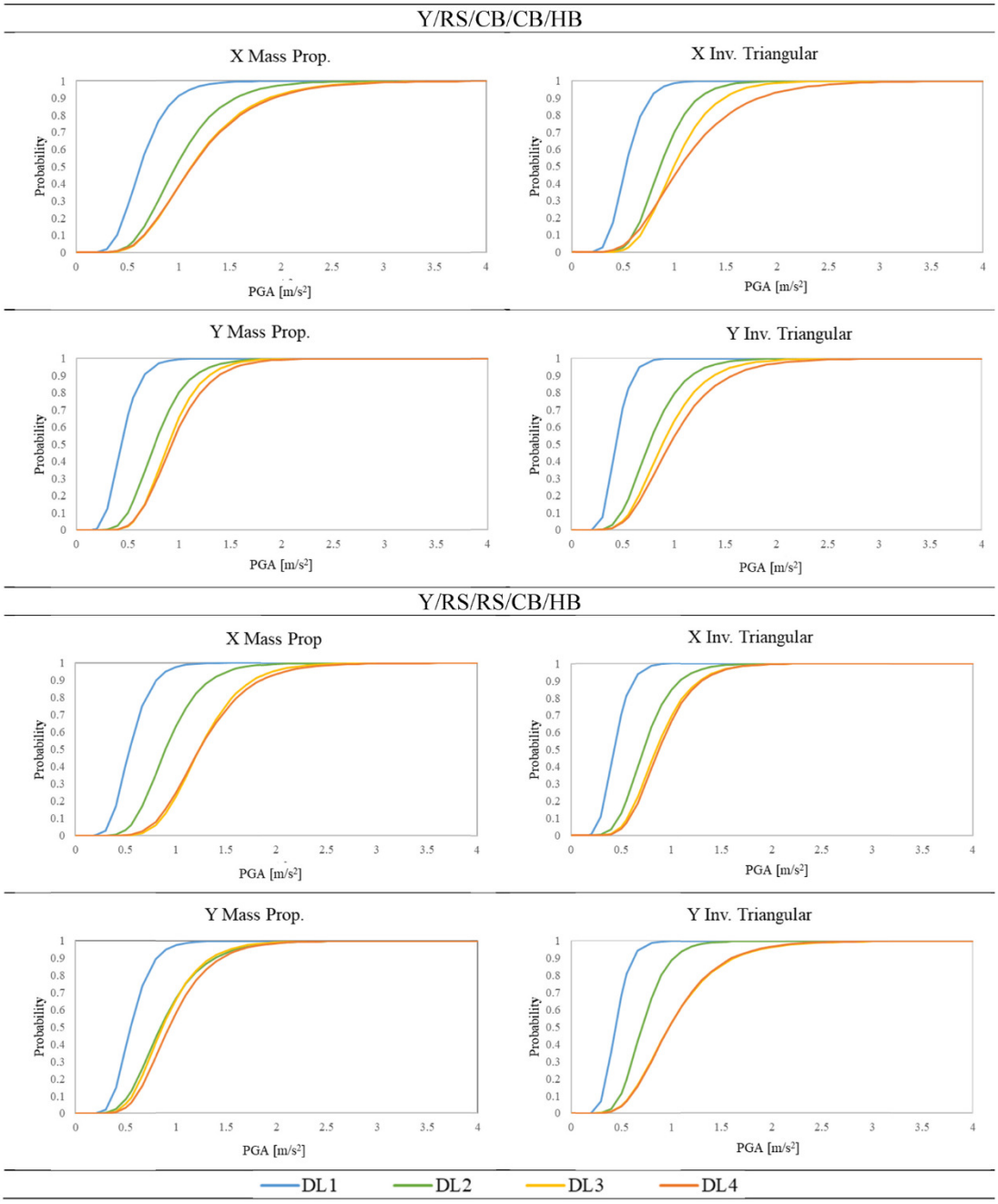

Fig. 15. The fragility curves for the two yes-lintel models.

Where the expression is fully described by (1) and the references made. In order to represent the *DS* by a binomial probability distribution, they can be described according to the following expressions:

$$p_{DS5}(im) = 0.8\left[1-\left(1-0.14\,\mu_{DS}^{1.4}\right)^{0.35}\right]p_{LS\,4}(im) \tag{6}$$

$$p_{DS\,4}(im) = p_{LS\,4}(im) - p_{DS5}(im) \tag{7}$$

$$\mu_{DS} = \sum_{1}^{4} p_{LS\,k} \tag{8}$$

Referring to the DS4, the definition of LS5 for its definition is a tough problem, related with the intrinsic assumptions of *near collapse*

for LS4 in the analytical formulations [64]. Finally, in order to complete the DS distribution, the probability of having a DS0 is described by:

$$p_{DS0}(im) = 1 - p_{LS\ 1}(im) = 1 - \Phi\left(\frac{\log\frac{im}{IM_{LS\ 1}}}{\beta_{LS\ 1}}\right) \tag{9}$$

The damage scenarios have been forecasted adopting the *DS* probability distribution of the derived fragility curves. Although the execution of nonlinear dynamic analyses is probably the more adequate tool to define the reliability of the seismic load patterns, in this work the criterium of the minimum *IM* value between the two different load patterns has been adopted. The inverse triangular pattern is attained for lower levels of PGA 24 times out of the total 32, while the mass proportional pattern achieves his thresholds first only 8 times. Concerning the *X* direction, the inverse triangular pattern achieves the *DLs* first in the 87.5% of the cases. Referring only to the last two *LSs*, it represents the 75% of the total amount. For the *Y* direction, the inverse triangular pattern is again the one achieving first

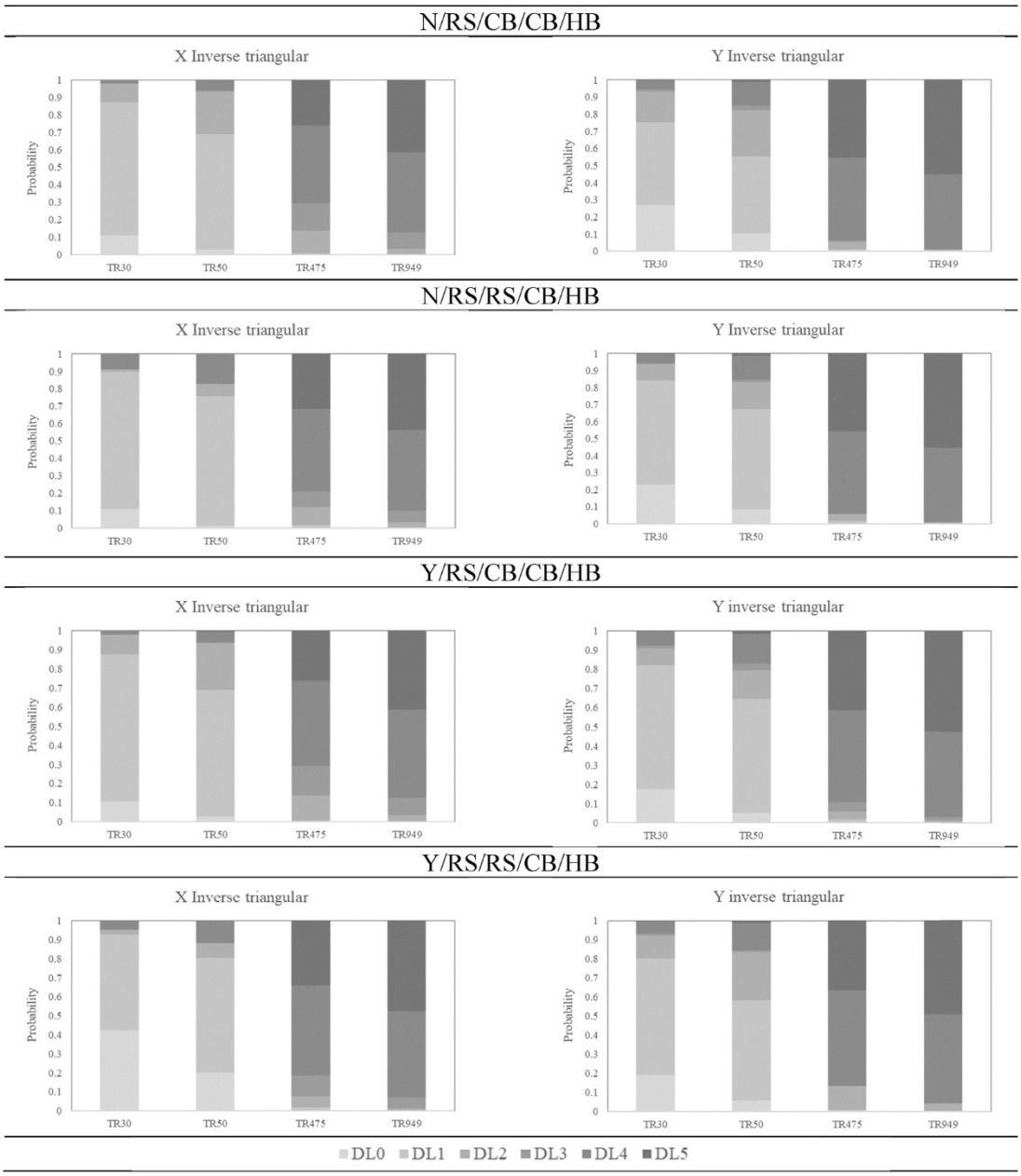

Fig. 16. Damage scenarios for the four different models according the four considered return periods.

the performance points (62.5% of the cases). Due to these reasons, in the presented work, the inverse triangular has been assumed for both directions. Following the statistically independence of the logic tree approach, for each branch the damage scenarios can be obtained, where each scenario represents the 25% of probability of occur given a seismic event. Considering the seismicity of Florence area, four different LSs associated with four Return Periods respectively have been assumed and associated to the different *DLs* (30, 50, 475 and 949 years). The return periods have been accounted on the basis of the Italian seismic code [4], considering a nominal life of the building equal to 50 years, with an important class equal to II (probability of exceedance in 50 years equal to 81% for SLO, 63% for SLD, 10% for SLV, 5% for SLC). Concerning the structure representative of the simple-block model, the results show a dual vulnerability. Specifically, the damage distributions describe inverse bell curves where the higher probabilities are expressed for the lowest and the highest *DLs*, avoiding the central *DSs*. This is due to the proximity of the fragility curves between the *PLs*, which also reflects the brittle behaviour of the model. Once the elastic range of the structures is completed, the degradation of the buildings in the plastic range is immediate and it rapidly leads to the highest *DSs*. In Fig. 16 the cumulative damage distributions of the models for the different return period are shown. Despite the models point out different probability distributions, the results exhibit the same global trend. Considering the *SLV* and *SLC*, the probability of exceedance the threshold *LS* are quite pronounced towards the *DL4* and *5*. For a seismic action of 475 years return period, in the *X* direction the four models show a probability concentrated between 44.5 and 47.7% to attain DL4. Lower values ranging around the 30% are given for *DL5* (except for model Y/RS/RS/CB/HB pointing out a 50.2% probability), which is the second probable LS. These percentages tend to increase for the *Y* direction, where the probability is mostly distributed between *DL4* and *DL5*. *DL4* distributions obtain values between 48.0% and 50.3%, while *DL5* is distributed in the range 38.8–45.7%. For the 949 years return period, the probabilities of *DL5* increase again, becoming the most probable damage class for earthquakes of such intensity. In *X* direction the probability of attain *DL4* rounds around the 45% for both directions. Then, *DL5* exhibits a probability between 41.2% and 56.7% in *X* (with a *mean* value of 47.5%), while in Y direction it denounces a less variations ranging between 50.5 and 55.3%. The fragility curves show a brittle behavior that highlights a particular seismic vulnerability. The analytical results obtained from the case study denounce a behaviour influenced by the technical and mechanical characteristics of the models. It is worth noting that, despite the presence of ring beams and rigid diaphragms allows a box behavior, it also interrupts the vertical alignments of the piers, promoting a storey mechanism which reduces the nonlinear capacity of the model [46]. This is an intrinsic characteristic for these buildings, which it must be considered. Other outcomes have been pointed out from the presented research; if the epistemic uncertainties resulted not so relevant in terms of sensitivity, this is mostly due by the floor level where they have been considered. In fact, the *EF* models are mostly characterized by a shear failure of the lowest levels, while the epistemic uncertainties dealt with the masonry typology disposition at the upper floors. This represents a structural characteristic. On the other side, the mechanical properties of the materials have been collected in a high-sensitivity class, denouncing the importance of the mechanical values in the performance variability.

4.4. *q-factor definition*

In addition, the structural behaviour factor q for the investigated building typology is provided. The q-factor represents an approximation of the ratio of the seismic forces that would invest the structure if its response was completely elastic. An extensive discussion about the *q-factor* values can be found in Magenes [76]. Namely, q is given by:

$$\boldsymbol{q} = \boldsymbol{q}_0\, \boldsymbol{k_r} \tag{10}$$

where $\boldsymbol{q}_0$ represents the ductility value and $\boldsymbol{k_r}$ depends by the vertical regularity of the construction (equal to 1 for regular structures, otherwise 0,8). The last Italian code for the existing URM buildings considers a $\boldsymbol{q}_0$ value equal to 1,75 OSR, increasing up to 2,5 OSR for masonry building with reinforced insertions [4]. This last term, the overstrength ratio (OSR) expresses the ratio between the base shear at ultimate displacement and the one reaching the plasticity in the first wall. The q-factor is assumed from the nonlinear analysis, as the ratio between the idealized maximum base shear $F_{el,\,max}$ and the one at the yielding point F_y :

$$q = \frac{F_{el,\,max}}{F_y} = q_0 \tag{11}$$

The Italian standards provide values for q-factor in case of linear elastic analysis. For the existing buildings the latter considers a q_0 value for URM equal to 1,75 OSR, increasing up to 2.5 OSR for masonry building with reinforced insertions [4]. This last term, the overstrength ratio (OSR) expresses the ratio between the base shear at ultimate displacement and the one reaching the plasticity in the first wall [77]:

$$q = \frac{F_{el,\,max}}{F_{el}} = \frac{F_{el,\,max}}{F_y}\frac{F_y}{F_{el}} = q_0\frac{F_y}{F_{el}} = q_0\, OSR \tag{12}$$

In this work, the values for both q_0 and *OSR* have been directly computed from the pushover analysis. In Fig. 17 the results for the q_0 values for the four different models are shown. Differences are pointed out especially within the two seismic load patterns rather than according to the two different directions. The *Y* direction denounces a slight lower value. Moreover, the mass proportional pattern leads to lower values of q_0, ranging between 1.33. On the other side, a mean value of 1.69 is obtained for the inverse triangular pattern. Complexly, they range from 1.28 to 1.86 with a mean value equal to 1.51. Concerning the definition of the OSR, the results present interesting outcomes (Fig. 18). The models without lintels exhibit low values of OSR; excluding the inverse triangular pattern in the *Y* direction, which it leads to OSR values between 1 and 1.07, the mean values of the two models without lintels for the other 6 combinations of seismic pattern and directions present a mean value equal to 2.35 and a standard deviation of 0.41. On the other side, the

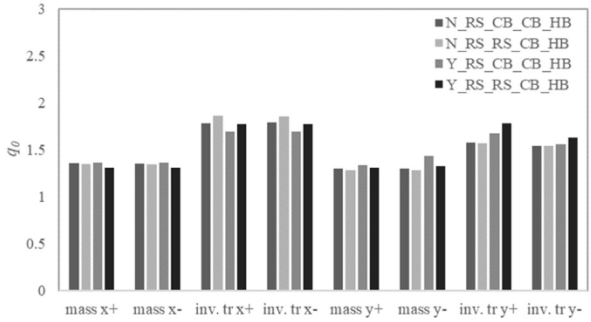

Fig. 17. Computation of the q_0 values according to the different models.

models with lintels, except for the mass proportional pattern in the *Y* direction, tend to exhibit OSR values smaller than 1,00.

For the models without lintels, the latter are coherent with other OSR values provided in the literature [76], on the other side, further studies (experimental and analytical) are needed concerning the yes-lintels models. This outcome can be justified by the different hierarchical roles defined inside the masonry panels. The models without lintels in the first linear phase are characterized by a less relevant damage diffusion, pointing out the attainment of the plasticity in earlier phases. The RC lintels over the opening allow a more diffuse localization of the damage along the masonry heights. Due to this, the shear or flexural strength of the panels is achieved only after that a higher number of panels already exploited their linear capacities. So, in terms of idealized bilinear curve, this attainment is given after the yielding points, defining no longer OSR increment coefficient.

This result points out outcomes that should dissuade in the choice of linear elastic analysis for the seismic vulnerability assessment of these buildings: the lack of knowledge about building details such as the presence of RC lintels over the openings can significantly alter the linear elastic response of the considered buildings. Therefore, unless of a univocal achieved knowledge, this method becomes unreliable.

5. Conclusive remarks

In this paper, the seismic vulnerability assessment of Florence's XX century masonry buildings has been investigated. The residential URM structures of the XX century constitute a relevant percentage of the Florentine stock deserving specific attention. The objective of this work has been pursued by means of urban data acquisition and numerical insights based on NLSA. The outcomes of the analytical procedure exhibited a relevant vulnerability of the buildings denouncing a brittle behaviour; considering the assumed hypothesis of homogeneity of the database, the same behaviour is expected for the other different structures. The sensitivity analysis conducted over the building model denounced relevant outcomes. In terms of vulnerability, although the different behaviours expressed by the pushover curves, the presence or not of the RC lintels over the openings does not significantly alter (or improve) the seismic vulnerability of those buildings. The epistemic uncertainties proved how easier assumptions could be accepted in the engineering practice, limiting the number of epistemic models and reducing the time consuming of the procedure. In that case, the aleatory ones indicate in the mechanical properties of the materials the main issues that need to be investigated. These results provide further information on the adoption of linear procedures in case of significant epistemic uncertainties, encouraging the usage of nonlinear constitutive models.

The analytical results are coherent with the post-earthquake evidence for modern structures as presented in Calderoni et al. [33] and Valluzzi et al. [34]. By comparing the analytical results with the empirical procedure presented in Cardinali et al. [35], this paper demonstrates the inadequacy of the empirical methodology adopted for the vulnerability assessment of the XX century URM buildings. It is worth noting that assuming the empirical rules of regularity, structural coherency and the presence of aseismic devices allows these buildings perfectly respond to what is considered a non-vulnerable building and a *box-behaviour* structure. Nonetheless, the presence of a ring beam leads to WPSS models where the shear capacity of the lowest storeys is demanded to the seismic resistance of

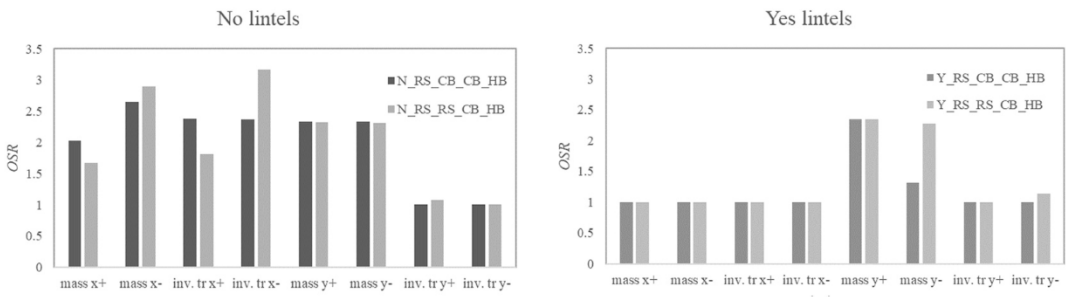

Fig. 18. Computation of the *OSR* values according to the different models.

the structure. Further studies are expected, aiming to define additional case studies for analytical assessment in order to assess the reliability of the previous assumptions; the evaluation of building with different heights is still beneficial, both with considerations about the role of irregularity. These further analyses would also regard the extension of the procedure to other classes of buildings and the implementation of the results at the urban scale through hybrid strategies. Finally, the research needs to continue evaluating strengthening solutions for the improvements of the safety of these structures and of the people who live in, as evaluations in terms of economic losses and risk-reduction policies.

Author statement

Vieri Cardinali: Conceptualization, Data curation, Formal analysis, Methodology, Investigation, Software, Visualization, Writing – original draft, Writing – review & editing.

Marco Tanganelli: Conceptualization, Project administration, Resources, Supervision, Writing – review & editing.

Rita Bento: Conceptualization, Supervision, Validation, Writing – review & editing.

Funding sources

This research did not receive any specific grant from funding agencies in the public, commercial, or not-for-profit sectors.

Declaration of competing interest

The authors declare that they have no known competing financial interests or personal relationships that could have appeared to influence the work reported in this paper.

Acknowledgements

The Authors thank CASA S.P.A. for the disposition and the interested towards the topics treated in this work and the archivists Elisabetta Bettio and Rita Romanelli for their support during the archive research.

Appendix A. Supplementary data

Supplementary data to this article can be found online at https://doi.org/10.1016/j.jobe.2022.104801.

References

[1] S. Martínez-Cuevas, M.B. Benito, J. Cervera, M.C. Morillo, M. Luna, Urban modifiers of seismic vulnerability aimed at Urban Zoning Regulations, Bull. Earthq. Eng. (2017), https://doi.org/10.1007/s10518-017-0162-2.
[2] Federal Emergency Management Agency, FEMA-356, Prestandard and Commentary for Seismic Rehabilitation of Buildings, 2000. Washington DC.
[3] EC 8-3 (2005). Design of Structures for Earthquake Resistance, Part 3: Strengthening and Repair of Buildings. European standard EN 1998-3. European Committee for Standardization (CEN), Brussels.
[4] NTC, L.L.P.P. Min, Aggiornamento delle «Norme tecniche per le costruzioni». G.U. No. 42 del 20 Febbraio D.M. Ministero Infrastrutture e Trasporti 17 gennaio 2018, 2018. Roma (in Italian).
[5] N. Lantada, J. Irizarry, A.H. Barbat, X. Goula, A. Roca, T. Susagna, L.G. Pujades, Seismic hazard and risk scenarios for Barcelona, Spain, using the Risk-UE vulnerability index method, Bull. Earthquake Eng. 8 (2) (2010) 201–229, https://doi.org/10.1007/s10518-009-9148-z.
[6] P. Lamego, P.B. Lourenço, M.L. Sousa, R. Marques, Seismic vulnerability and risk analysis of the old building stock at urban scale: application to a neighbourhood in Lisbon, Bull. Earthq. Eng. 15 (2017) 2901–2937, https://doi.org/10.1007/s10518-016-0072-8.
[7] M. Dolce, A. Prota, B. Borzi, F. da Porto, S. Lagomarsino, Moroni C. Magenes, A. Penna, M. Polese, E. Speranza, G.M. Verderame, G. Zuccaro, Seismic risk assessment of residential buildings in Italy, Bull. Earthq. Eng. (2020), https://doi.org/10.1007/s10518-020-01009-5.
[8] J. Milosevic, R. Bento, S. Cattari, 3DGIS representation for supporting seismic mitigation policies at urban scale: the 775case study of Lisbon, J. Cult. Herit. (2020), https://doi.org/10.1016/j.culher.2020.04.001.
[9] A.G. Simões, R. Bento, S. Lagomarsino, S. Cattari, P.B. Lourenço, Seismic assessment of nineteenth and twentieth centuries URM buildings in Lisbon: structural features and derivation of fragility curves, Bull. Earthq. Eng. 18 (2020) 645–672, https://doi.org/10.1007/s10518-019-00618-z.
[10] M. Dolce, A. Prota, Guest editorial to the special issue—Seismic risk assessment in Italy, Bull. Earthq. Eng. 19 (2021) 2995–2998, https://doi.org/10.1007/s10518-021-01107-y.
[11] R. Maio, T.M. Ferreira, J.M. Estêvão, B. Pantò, I. Calio, R. Vicente, Seismic performance-based assessment of urban cultural heritage assets through different macroelement approaches, J. Build. Eng. 29 (2020), 101083.
[12] G.M. Calvi, R. Pinho, G. Magenes, J.J. Bommer, L.F. Restrepo-Vélez, H. Crowley, Development of seismic vulnerability assessment methodologies over the past 30 years, ISET J. Earthq. Technol. 43 (2006) 75–104, https://doi.org/10.1016/j.asej.2020.04.001, 2006.
[13] R. Vicente, S. Parodi, S. Lagomarsino, H. Varum, J.A.R. Mendes Silva, Seismic vulnerability and risk assessment: case study of the historic city centre of Coimbra, Portugal, Bull. Earthq. Eng. 9 (2011) 1067–1096, https://doi.org/10.1007/s10518-010-9233-3, 2011.
[14] Pitilakis, K., Crowlery, H., Kaynia, A.M., (2014) (eds.), SYNER-G: Typology Definition and Fragility Functions for Physical Elements at Seismic Risk, Geotechnical, Geological and Earthquake Engineering 27, DOI 10.1007/978-94-007-7872-6_5, © Springer Science+Business Media Dordrecht 2014.
[15] M.M. Kassem, F.M. Nazri, E.N. Farsangi, The seismic vulnerability assessment methodologies: a state-of-the-art review, Ain Shams Eng. J. (2020), https://doi.org/10.1016/j.asej.2020.04.001.
[16] A. Sandoli, G.P. Lignola, B. Calderoni, A. Prota, Fragility curves for Italian URM buildings based on a hybrid method, Bull. Earthq. Eng. 19 (2021) 4979–5013, https://doi.org/10.1007/s10518-021-01155-4.
[17] N. Augenti, F. Parisi, Learning from construction failures due to the 2009 L'Aquila, Italy, earthquake, J. Perform. Constr. Facil. 24 (6) (2010) 536–555, 2010.
[18] F. Parisi, F. De Luca, F. Petruzzelli, R. De Risi, E. Chioccarelli, I. Iervolino, Field inspection after the may 20thand 29th2012 Emilia-Romagna earthquakes, available on, http://www.reluis.it, 2012.
[19] GL-INGV [Gruppo di Lavoro INGV sul terremoto di Amatrice], Secondo rapporto di sintesi sul Terremoto di Amatrice Ml 6.0 del 24 Agosto 2016, Italia Centrale) (2016), https://doi.org/10.5281/zenodo.154400 (in Italian).

[20] ISTAT, General Population and Housing Census, 2001. http://www.dawinci.istat.it/pop.
[21] M. Tanganelli, T. Rotunno, V. Cardinali, S. Viti, Public housing in florence: seismic assessment of masonry buildings, Procedia Struct. Integr. 11 (2018) 266–273, https://doi.org/10.1016/j.prostr.2018.11.035.
[22] D. Molin, A. Paciello, Seismic hazard assessment in Florence city Italy, J. Earthq. Eng. 3 (4) (1999) 475–494, https://doi.org/10.1080/13632469909350356.
[23] A. Rovida, M. Locati, R. Camassi, B. Lolli, P. Gasperini, Catalogo Parametrico dei Terremoti Italiani, release 2015, INGV, 2016, 2016, https://emidius.mi.ingv.it/CPTI15-DBMI15/description_CPTI15.htm.
[24] G. Correia Lopes, R. Vicente, T.M. Ferreira, M. Azenha, Intervened URM buildings with RC elements: typological characterisation and associated challenges, Bull. Earthq. Eng. 17 (2019) 4987–5019, https://doi.org/10.1007/s10518-019-00651-y.
[25] P.G. Touliatos, Seismic behaviour of traditionally-built constructions: repair and strengthening, in: Courses and Lectures-International Centre for Mechanical Sciences, Springer, New York, 1996, pp. 57–70.
[26] (2015). Masonry box behavior. in Lourenço, P. (2015) R. Marques, Masonry modeling, in: Michael Beer, Ioannis A. Kougioumtzoglou, Edoardo Patelli, Siu-Kui Au (Eds.), Encyclopedia of Earthquake Engineering, Springer Berlin Heidelberg, Berlin, Heidelberg, 2015, pp. 1419–1431, https://doi.org/10.1007/978-3-642-35344-4_153.
[27] A. Sandoli, B. Calderoni, Assessment of the seismic vulnerability at territorial scale: a new structural classification of existing buildings and definition of fragility curves, in: Proceedings of 10th International Masonry Conference (IMC), 2018. Milano.
[28] RD 1909, n Royal Decree, Technical and Hygienic Rules for Repairs, Reconstructions and New Constructions of Private and Public Buildings in the Zones Affected by 28th December 1908 Earthquakes, and in Precedent Ones, 193, Italian Government, 22 Apr 1909 (in Italian).
[29] RD 1937, n Royal Decree, Technical Rules for Constructions, with Particular Prescriptions for Zones Hit by Earthquake, Italian Government, 2015, 27 Dec 1937 (in Italian).
[30] K. Beyer, S. Petry, M. Tondelli, A. Paparo, Towards displacement-based seismic design of modern unreinforced masonry structures, Geotech. Geol. Earthquake Eng. (2014) 401–428, https://doi.org/10.1007/978-3-319-07118-3_12.
[31] K. Beyer, M. Tondelli, F. Vanin, S. Petry, A. Paparo, Seismic behaviour of unreinforced masonry buildings with reinforced concrete slabs: Assessment of in-plane and out-of-plane response, Earthquake Engineering & Structural Dynamics Laboratory (EESD), École Polytechnique Fédérale de Lausanne, 2015 (EPFL) April 2015.
[32] A. Penna, P. Morandi, M. Rota, C.F. Manzini, F. Da Porto, G. Magenes, Performance of masonry buildings during the Emilia 2012 earthquake, Bull. Earthq. Eng. 12 (2014) 2255–2273, https://doi.org/10.1007/s10518-013-9496-6.
[33] B. Calderoni, E.A. Cordasco, M. Del Zoppo, A. Prata, Damage assessment of modern masonry buildings after the L'Aquila earthquake, Bull. Earthq. Eng. 18 (2020) 2275–2301, https://doi.org/10.1007/s10518-020-00784-5, 2020.
[34] M.R. Valluzzi, L. Sbrogiò, Y. Saretta, Intervention strategies for the seismic improvement of masonry buildings based on FME validation: the case of a terraced building struck by the 2016 Central Italy earthquake, Buildings 11 (9) (2021) 404, https://doi.org/10.3390/buildings11090404.
[35] V. Cardinali, S. Viti, M. Tanganelli, in: M. Papadrakakis, M. Fragiadakis (Eds.), Seismic Vulnerability of the Residential Buildings of Florence, COMPDYN 2019 7th ECCOMAS Thematic Conference on Computational Methods in Structural Dynamics and Earthquake Engineering, Crete, Greece, 24–26 June 2019, 2019.
[36] S.S.N. Gruppo Nazionale per la Difesa dai Terremoti - GNDT-, Scheda di esposi-zione e vulnerabilità e di rilevamento danni di primo e secondo livello (muratura e c. a.), Gruppo Nazionale per la Difesa dai Terremoti, Rome, 1994 (in Italian).
[37] MIT, Circolare 21 gennaio 2019, n. 7 Istruzioni per l'applicazione dell'«Aggiornamento delle "Norme tecniche per le costruzioni"» di cui al decreto ministeriale 17 gennaio 2018, 2019. G.U. n. 47 del 26/02/2009, Supplemento Ordinario n. 27, Rome, (in Italian).
[38] S. Bracchi, M. Rota, G. Magenes, A. Penna, Seismic assessment of masonry buildings accounting for limited knowledge on materials by Bayesian updating, J. Bull. Earthquake Eng. 14 (8) (2016) 2273–2297, https://doi.org/10.1007/s10518-016-9905-8.
[39] J. Milosevic, S. Cattari, R. Bento, Sensitivity analysis of the seismic performance of ancient mixed masonry-RC buildings in Lisbon, Int. J. Magn. Reson. Imag. 3 (2) (2018) 108–154.
[40] S. Boschi, L. Galano, A. Vignoli, Mechanical characterisation of Tuscany masonry typologies by in situ tests, 2019, Bull. Earthq. Eng. 17 (2019) 413–438, https://doi.org/10.1007/s10518-018-0451-4.
[41] M.T. Cristofaro, S. Viti, M. Tanganelli, New predictive models to evaluate concrete compressive strength using the sonreb method, J. Build. Eng. (2019), 100962, https://doi.org/10.1016/j.jobe.2019.100962.
[42] M.T. Cristofaro, A. D'Ambrisi, M. De Stefano, Nuovi modelli previsionali per la stima della resistenza a compressione del calcestruzzo con il metodo Sonreb, in: Bologna ANIDIS (Ed.), 28 Giugno- 2 Luglio 2009, 2009, pp. 0–0, ISBN:9788890429200 (in Italian).
[43] G.M. Verderame, A. Stella, E. Cosenza, Le proprietà meccaniche degli acciai impiegati nelle strutture in cemento armato realizzate negli anni '60, X Convegno Nazionale "L'Ingegneria Sismica in Italia, in: Potenza e Matera 9-13 Settembre 2011 (in Italian), 2011.
[44] S. Lagomarsino, A. Penna, A. Galasco, S. Cattari, TREMURI program: an equivalent frame model for the nonlinear seismic analysis of masonry buildings, Eng. Struct. 56 (2013) 1787–1799.
[45] A. Penna, S. Lagomarsino, A. Galasco, A nonlinear macroelement model for the seismic analysis of masonry buildings, Earthq. Eng. Struct. Dynam. 43 (2) (2014) 159–179.
[46] S. Cattari, S. Lagomarsino, Seismic assessment of mixed masonry-reinforced concrete buildings by non-linear static analyses, Earthq Struct 4 (3) (2013) 241–264.
[47] S. Lagomarsino, D. Camilletti, S. Cattari, S. Marino, Seismic assessment of existing irregular masonry buildings by nonlinear static and dynamic analyses, in: K. Pitilakis (Ed.), Recent Advances in Earthquake Engineering in Europe. ECEE 2018., Geotechnical, Geological and Earthquake Engineering, 46, Springer, Cham, 2018.
[48] K. Beyer, A. Dazio, Quasi-static cyclic tests on masonry spandrels, Earthq. Spectra 28 (3) (2012) 907–929.
[49] S. Petry, K. Beyer, Cyclic test data of six unreinforced masonry walls with different boundary conditions, Earthq. Spectra (2014). https://doi.org/10.1193/101513eqs269.
[50] P. Morandi, L. Albanesi, F. Graziotti, T. Li Piani, A. Penna, G. Magenes, Development of a dataset on the in-plane experimental response of URM piers with bricks and blocks, Construct. Build. Mater. (2018). https://doi.org/10.1016/j.conbuildmat.2018.09.070.
[51] J. Milosevic, R. Bento, S. Cattari, Definition of fragility curves through nonlinear static analyses: procedure and application to a mixed masonry-RC building stock, Bull. Earthq. Eng. 18 (2019) 513–545, https://doi.org/10.1007/s10518-019-00694-1, 2019.
[52] V. Turnšek, F. Cacovic, Some experimental results on the strength of brick masonry walls, in: Proc. Of the 2nd International Brick Masonry Conference, 1970, pp. 149–156.
[53] R. Marques, P.B. Lourenço, Unreinforced and confined masonry buildings in seismic regions: validation of macro-element models and cost analysis, Eng. Struct. 64 (2014) 52–67.
[54] J. Haddad, S. Cattari, S. Lagomarsino, Use of the model parameter sensitivity analysis for the probabilistic- based seismic assessment of existing buildings, J. Bull. Earthq. Eng. 17 (2019) 1983–2009. https://doi.org/10.1007/s10518-018-0520-8.
[55] O. Palermo, V. Cardinali, M.R. Azzara, M. Tanganelli, Valutazione delle prestazioni strutturali di edifici residenziali pubblici: due insediamenti INA CASA a Firenze, VII Convegno Internazionale ReUSO Matera, 2019, pp. 23–26. Ottobre 2019 (in Italian).
[56] C. Michel, A. Karbassi, P. Lestuzzi, Evaluation of the seismic retrofitting of an unreinforced masonry building using numerical modeling and ambient vibration measurements, Eng. Struct. 158 (2018) 124–135, https://doi.org/10.1016/j.engstruct.2017.12.016.
[57] D. Sivori, M. Lepidi, S. Cattari, Ambient vibration tools to validate the rigid diaphragm assumption in the seismic assessment of buildings, Earthq. Eng. Struct. Dynam. 49 (2020) 194–211, 2020.
[58] R. Maio, G. Tsionis, Seismic fragility curves for the European building stock: review and evaluation of analytical fragility curves, in: EUR 27635 EN. European Laboratory for Structural Assessment, Institute for the Protection and Security of the Citizen, Joint Research Centre of the European Commission, Ispra (Italy), 2015.

[59] M. Rota, A. Penna, G. Magenes, A methodology for deriving analytical fragility curves for masonry buildings based on stochastic nonlinear analyses, Eng. Struct. 32 (5) (2010) 1312–1323, https://doi.org/10.1016/j.engstruct.2010.01.009. Elsevier Ltd.
[60] M. Remki, F. Kehila, Analytically derived fragility curves and damage assessment of masonrybuildings, in: H. Rodrigues, A. Elnashai, G. Calvi (Eds.), Facing the Challenges in Structural Engineering. GeoMEast 2017. Sustainable Civil Infrastructures, Springer, Cham, 2018, https://doi.org/10.1007/978-3-319-61914-9_4.
[61] G.M. Calvi, A displacement-based approach for vulnerability evaluation of classes of buildings, J. Earthq. Eng. 3 (3) (1999) 411–438.
[62] S. Lagomarsino, S. Cattari, PERPETUATE guidelines for seismic performance-based assessment of cultural heritage masonry structures, Bull. Earthq. Eng. 13 (1) (2015) 13–47.
[63] J. Douglas, D.M. Seyedi, T. Ulrich, H. Modaressi, E. Foerster, K. Pitilakis, D. Pitilakis, A. Karatzetzou, G. Gazetas, E. Garini, M. Loli, Evaluation of seismic hazard for the assessment of historical elements at risk: description of input and selection of intensity measures, Bull. Earthq. Eng. 13 (1) (2014) 49–65, https://doi.org/10.1007/s10518-014-9606-0.
[64] S. Lagomarsino, S. Cattari, Fragility functions of masonry buildings, in: SYNER-G: Typology Definition and Fragility Functions for Physical Elements at Seismic Risk, Springer, 2014, pp. 111–156.
[65] M.A. Erberik, Generation fragility curves for Turkish masonry buildings considering in-plane failure modes, Earthq. Eng. Struct. Dynam. 37 (2008) 387–405.
[66] P.B. Lourenço, D.V. Oliveira, J.C. Leite, J.M. Ingham, C. Modena, F. Da Porto, Simplified indexes for the seismic assessment of masonry buildings: International database and validation, Eng. Fail. Anal. 34 (2013) 585–605, https://doi.org/10.1016/j.engfailanal.2013.02.014.
[67] E. Cescatti, P. Salzano, C. Casapulla, F. Ceroni, F. Da Porto, A. Prota, Damages to masonry churches after 2016–2017 Central Italy seismic sequence and definition of fragility curves, Bull. Earthq. Eng. 18 (2020) 297–329, https://doi.org/10.1007/s10518-019-00729-7.
[68] S.A. Freeman, The capacity spectrum method as a tool for seismic design, in: Proceedings of 11th European Conference of Earthquake Engineering, 1998. Paris, France.
[69] P. Fajfar, Capacity spectrum method based on inelastic spectra, Earthq. Eng. Struct. Dyn28 (9) (1999) 979–993.
[70] S. Marino, S. Cattari, S. Lagomarsino, Are the nonlinear static procedures feasible for the seismic assessment of irregular existing masonry buildings? Eng. Struct. 200 (2019) https://doi.org/10.1016/j.engstruct.2019.109700.
[71] P.E. Pinto, R. Giannini, P. Franchin, Seismic Reliability Analysis of Structures, IUSS Press, Pavia, 2004, ISBN 88-7358-017-3.
[72] CNR-DT212, Guide for the Probabilistic Assessment of the Seismic Safety of Existing Buildings), Consiglio Nazionale delle Ricerche, Rome, Italy, 2013 (in Italian).
[73] I. Iervolino, C. Galasso, E. Cosenza, REXEL: computer aided record selection for code-based seismic structural analysis, Bull. Earthq. Eng. 8 (2) (2009) 339–362, https://doi.org/10.1007/s10518-009-9146-1.
[74] E.S.M. working group, European Strong-Motion database, version 0.1, Network Activity 3: networking acceleration networks and SM data users, Project NERA (2015). URL, www.nera-eu.org, http://esm.mi.ingv.it.
[75] S. Cattari, S. Lagomarsino, V. Bosiljkov, D. D'Ayala, Sensitivity analysis for setting up the investigation protocol and defining proper confidence factors for masonry buildings, Bull. Earthq. Eng. 13 (1) (2014) 129–151, https://doi.org/10.1007/s10518-014-9648-3.
[76] G. Magenes, Masonry building design in seismic areas: recent experiences and prospects from a European standpoint, in: Keynote 9, 1st European Conference on Earthquake Engineering and Engineering Seismology, 3-8 September 2006, Geneva, Switzerland, CD-ROM, 2006, 2006.
[77] G. Magenes, P. Morandi, Some issues on seismic design and assessment of masonry buildings based on linear elastic analysis, in: Proc. Of the Michael John Nigel Priestley Symposium, IUSS Press, Pavia, Italy, 2008, pp. 83–94. July 2008.